University of Groningen

university of groningen

Faculty of Science and Engineering

Seabed conditions and its relation to Suction Anchor Operation

Bachelor Thesis - Integration Project
Industrial Engineering & Management

June - 2020

Author:
Nick van Dijken
S3211754

Supervisors:
Prof. Dr. A. Vakis
Ir. T.M. Kousemaker

Abstract

The company Ocean Grazer B.V. has developed a design for a modular, renewable energy source based primarily on wave energy. Additionally, a design was developed that allowed for excess energy to be converted into potential, mechanical energy, promptly named: “Ocean Battery”. The Ocean Battery is to be released into the ocean, where it will sink to the bottom and anchor itself to the seafloor by means of suction anchors. The Ocean Battery will be connected to the main installation by means of numerous cables, which allows the main installation to exist as a floating construction. The Ocean Battery however, will feature a bladder with which excess energy will be captured, using a turbine powered by excess energy to fill this bladder with water. When this energy is required again, the pressure from the ocean above will press the water inside the bladder back through a turbine, regaining the potential energy that was stored.

For this design to function properly, the Ocean Battery is to be properly secured and anchored to the ocean floor by means of aforementioned suction anchors. The conditions and configurations required to guide this operation properly, differs based on the location and composition of the ocean floor to which the Ocean Battery will anchor itself. Therefore, this thesis aims to analyse a multitude of different seafloor conditions so that guidelines can be formulated for each set of conditions. This will allow the Ocean Battery to be deployed in almost any circumstance.

Table of Contents

List of Symbols

In order of moment of encounter

P	Penetration Resistance
W'	Effective weight
s	Suction force
D	Mean caisson diameter
D_o	Caisson Diameter - outside
D_i	Caisson Diameter - inside
h	Depth
α_o	Adhesion factor - outside
α_i	Adhesion factor - inside
s_{uo}	Shear strength at mudline
s_{u1}	Average shear strength over depth of skirt
s_{u2}	Shear strength at caisson skirt tip
γ'	Effective unit weight of soil
γ_w	Unit weight of water
t	Caisson wall thickness
N_q	Overburden Bearing Capacity Factor
N_c	Cohesion Bearing Capacity Factor
N_γ	Self-weight Bearing Capacity Factor
ρ	Shear strength rate of change
N_c^*	Bearing Capacity Factor for uplift of buried circular footing
K	Vertical to horizontal stress factor
δ	Interface friction angle of soil
Z_o	Outer Z-term
Z_i	Inner Z-term
σ'_{end}	Collective effective stress
σ'_{vo}	Outer effective vertical stress
σ'_{vi}	Inner effective vertical stress
A_i	Inside area of caisson
k_f	Ratio between inside- and outside permeability
φ'	Effective internal angle of friction
Q	Undrained holding capacity in cohesive soils
Q_{so}	Side shear stress on outside wall of caisson
Q_b	Tensile bearing capacity of foundation soil
W_c	Submerged weight of caisson
W_s	Submerged weight of soil plug
Q_{sum}	Sum of Q_{so}, Q_b and W_s
H	Depth of tip of caisson
α	Friction factor

f	Bearing Capacity correction coefficient
D_r	Length of diagonal for rectangular caissons
H_c	Undrained holding capacity in non-cohesive soils
$R_{s(OS)}$	Frictional resistance between soil and outer caisson skirt
$R_{s(IS)}$	Frictional resistance between soil and inner caisson skirt
R_{sum}	Sum of $R_{s(OS)}$, $R_{s(IS)}$ and W_s

1. Introduction

The company Ocean Grazer B.V. along with the research group Computational Mechanical and Materials Engineering (CMME) are developing innovative energy solutions primarily focussed on offshore wave and wind energy (Ocean Grazer, 2020). They have developed a multitude of scale-models that simulate how their modular designs function. The company has categorized their projects in three hybrid sections: Ocean Power, which focuses on power generation through wave and wind energy, Ocean Battery, which focuses on the storage of excess energy, and lastly Ocean Foundation, the structures that will facilitate the support of the other two modules.

The company has opted to use suction anchors to anchor their installation to the ocean floor safely. Suction Anchors, otherwise known as suction caissons, have been employed traditionally by the gas and oil industry, yet are now also used as a solution for placing offshore renewable energy sources such as wind turbines (Byrne et al, 2002). Suction caissons are in most cases cheaper and more effective than traditional ocean floor installations, such as pile foundations where large piles are brought into the ocean floor so that they may serve as a foundation for structures. Additionally, suction caissons can be removed relatively easily, are more environmentally friendly and generate less noise during installation, amongst other benefits (van Dijk, 2018).

Suction caissons are usually cylindrical anchors that are released so that they sink down to the ocean floor. Here, the weight will cause initial insertion into the ocean floor whilst captured water is free to be drained through the top of the anchor. The bottom of the anchor is completely open, and will thus allow water and initial sediment to enter the anchor. What ensues is the attachment of a pump to the top of the anchor, which will actively pump water out of the internal structure of the anchor. By doing this, an underpressure is created inside the anchor. This pressure difference will create a “suction”-effect, causing the anchor to drive itself deeper into the ocean floor as more water is being pumped out (Zhou et al, 2006). Figure 1 features a simplified model of the installation of a suction caisson into the ocean floor.

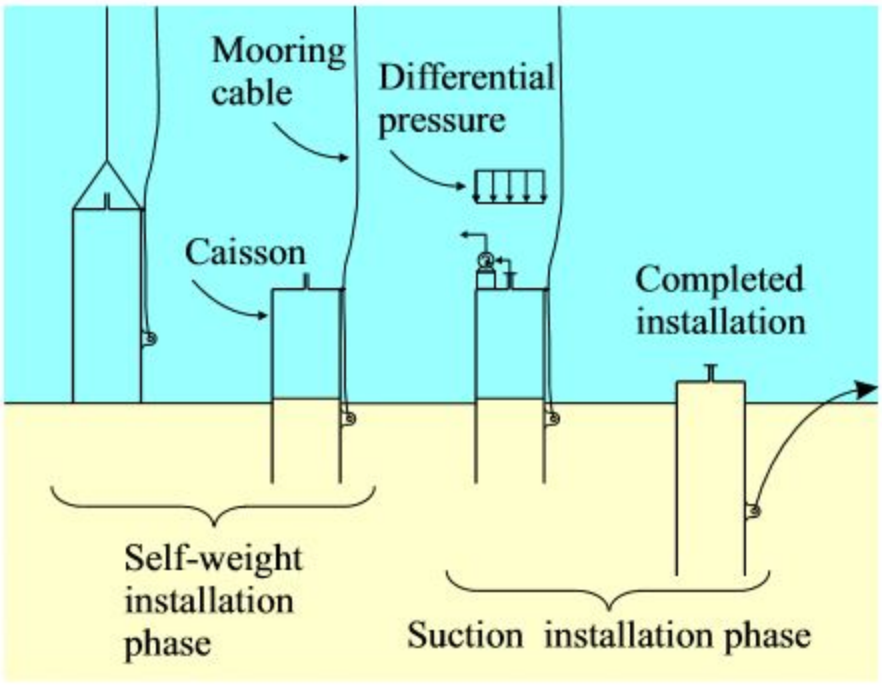

Figure 1. Suction Caisson installation process (Chaudhari et al, 2018)

When the caisson has been properly anchored into the ocean floor, the pump at the top is closed. A load may now be applied on the caisson such as a structure. The caisson can be uninstalled quite easily by applying an overpressure, effectively pushing the anchor upward.

The proper installation and operation of a suction caisson depends on a multitude of factors. These factors can be categorized under either ocean floor factors or suction anchor factors. Properties of the soil in which installation takes place, have an effect on both the installation procedure and operation phase of the anchor (Harireche et al, 2013). This research will aim to clearly display how these two sets of properties affect both the installation phase and operation phase of the Ocean Foundation prototype.

2. Problem Analysis

2.1 Problem Statement

Properly installing a suction caisson foundation structure requires analysis of the ocean floor to determine its properties. Currently, there is no clear overview of how different soil compositions react with the prototype Ocean Grazer setup. Additionally, their set-up of suction caissons comes with unique issues. The Ocean Battery is to be anchored to the ocean floor utilising 9 suction caissons which will exist close to one another. Depending on the soil in which they will anchor themselves, the operation of one caisson may influence or obstruct the operation of another, or the joint operation of all 9 caissons together could cause soil liquefaction amongst other problems. Ideally, known problems with specific soil types could be highlighted and incorporated at the start of installation.

Through analysis of multiple ocean floor compositions and their effects on the suction caisson installation operation, a range of different results can be compared so that the performance of the Ocean Foundation can be described.

Therefore, the problem is formulated as follows:
There is a need for knowledge concerning the effects of ocean floor compositions on suction caisson operations, in order to properly configure the proposed suction caisson prototype for installation and operation given a multitude of different soils.

2.2 Stakeholder Analysis

Multiple stakeholders and a problem owner are identified with relation to the aforementioned problem statement. Firstly, W.A. Prins is identified as the problem owner, as he is a co-founder of the company. Therefore, the success and applicability of Ocean Grazer projects, among which the Ocean Foundation projects, is of much interest to him. Additionally, we identify A. Vakis, co-founder and Scientific Advisor of Ocean Grazer B.V., as a second key player. The analysis of the ocean floor and its significance to the deployment and success of the Ocean Battery and its components are directly related to him. Thirdly, we identify M. van Rooij as a stakeholder. He is co-founder and current Chief Technology Officer (CTO) of the company, making him directly responsible for the set-up and supply of experiments and models. Small-scale models of prototype suction caissons are currently used by the company to simulate conditions of the ocean floor. Due to his responsibility and stake regarding the success of the company and deployment of the Ocean Batteries, van Rooij is identified as a third key player.

Lastly, we identify the research group Computational Mechanical and Materials Engineering (CMME) as a stakeholder. The research group is directly related to the University of Groningen, Faculty of Science and Engineering, of which A. Vakis and W.A. Prins are members. As a research group of the university, their interest remains high regarding the successful application of Ocean Grazer products. However, their power within the company itself is respectively low.

Therefore, CMME should be informed regularly regarding the progress of the company's innovations.

2.3 System Description

As mentioned before, the Ocean Grazer's product will be entirely modular, with several different modules that feature either energy production or energy storage systems. The three key modules are Ocean Power, which includes energy generation solutions, the Ocean Battery, which stores energy, and the Ocean Foundation, which anchors the Ocean Battery to the ground. Other modules feature the possibility of adding i.e. Wind Turbines and Solar Panels, either to be directly anchored to the soil or placed in a floating structure for deep-sea application. A model of the current design can be seen in Figure 2.

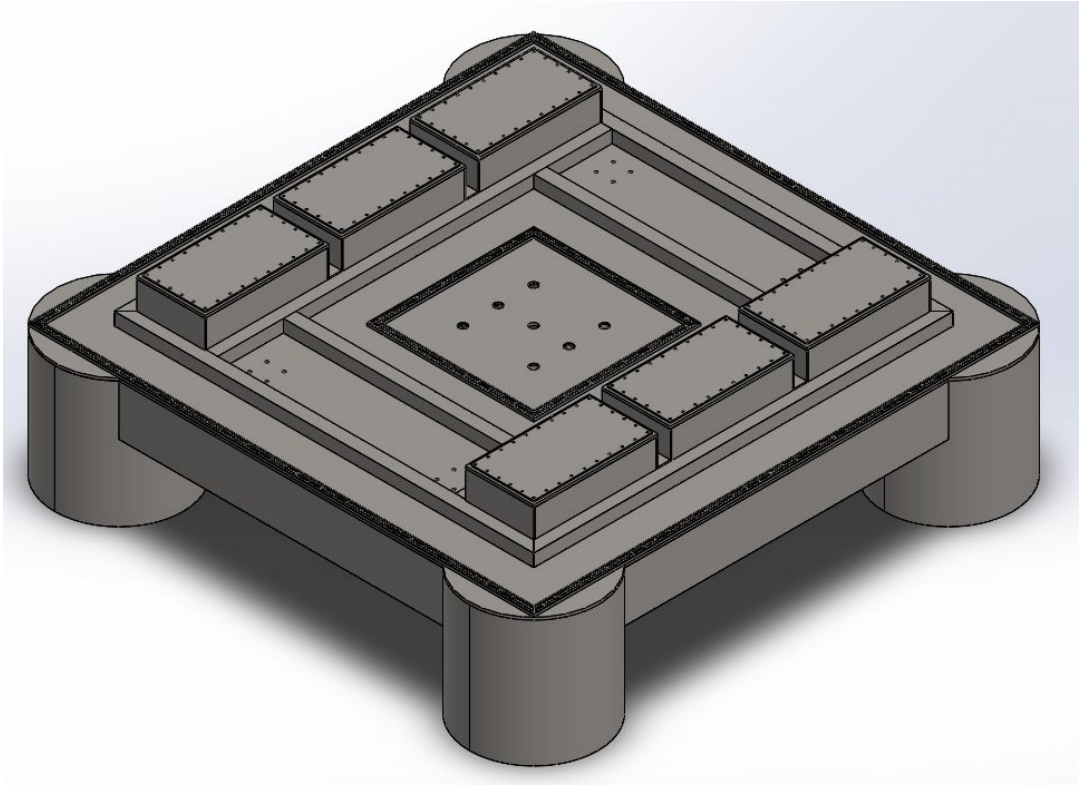

Figure 2. Current Ocean Foundation model **(Ocean Grazer, 2020)**

The aforementioned Ocean Battery module will feature an energy storage system, which will rest on the Ocean Foundation. It features an internal pressure structure mostly consisting of concrete. The top of the Ocean Battery features a rubber "bladder" that is designed to hold (fresh-) water, which serves the purpose of storing potential energy. A cross-section of the current prototype Ocean Battery model is shown in Figure 3. Excess energy generated by the Ocean Energy modules is sent downward to the Ocean Battery which is anchored directly to the ocean floor by means of suction caissons. Here, this excess energy will be used to power a pump that will pump internal fresh water into the aforementioned rubber bladder. In doing so, electrical energy is converted into mechanical, potential energy. To extract this energy after it

has been stored, the immense pressure of the ocean above will cause the bladder to deflate, pushing the fresh water back through a turbine which will convert the potential energy back into electrical energy, which can then be sent to an external energy grid (Ocean Grazer, 2020;van der Loo, 2020).

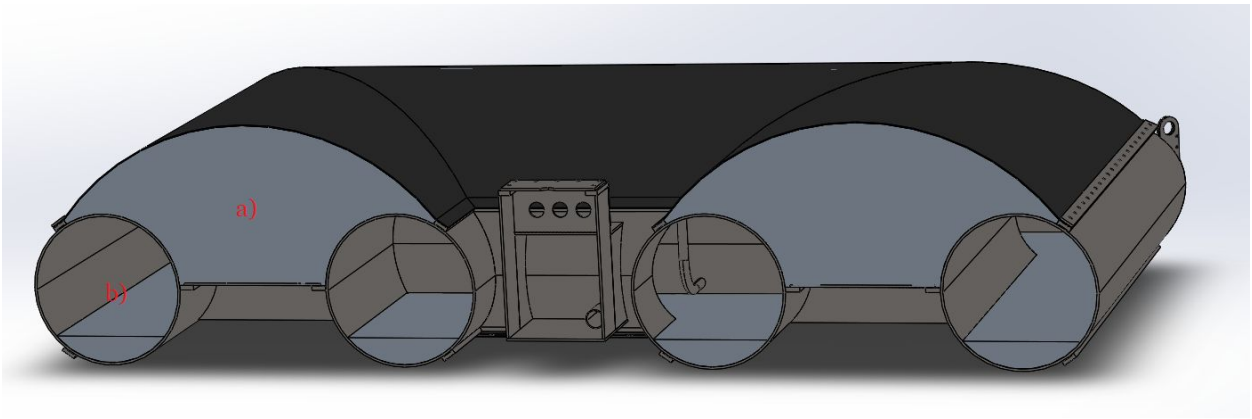

Figure 3. Cross-section of the current Ocean Battery model (Ocean Grazer, 2020). Section a) displays the rubber bladder whereas section b) displays the water reservoir.

This research will look at two separate phases as identified by Ocean Grazer and detailed by my predecessor K. van der Loo earlier this year (van der Loo, 2020). Each phase has a specific relation concerning the ocean floor soil and each phase is tied to specific problems. Figure 4 details a schematic visualization of the installation phase and the operating phase.

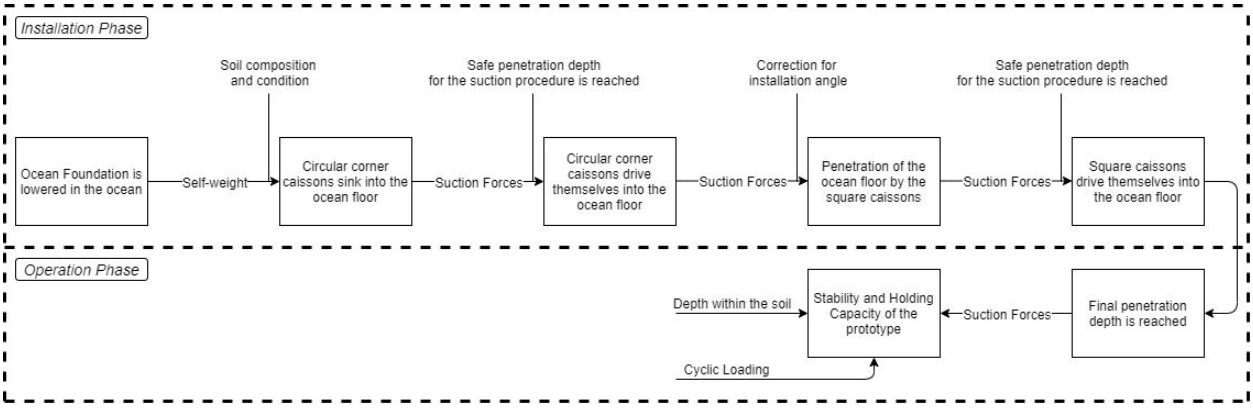

Figure 4. Ocean Foundation operation phases (Ocean Grazer, 2020)

Thus, each system will be subject to specific problems which partly depend on soil conditions, and partly on the properties of the anchor itself. Both sets of properties will determine how the suction anchors must be configured, and which problems are prone to occur.

3. Research Design

3.1 Design Goal

Currently, a lack of knowledge exists concerning the performance of the Ocean Foundation in different oceanic soils. During both the installation and operation phase, properties of the soil will determine how well the current prototype performs. The prototype's performance will be tested during self-weight installation and suction-assisted installation as well as its ability to correct its own angle with respect to the soil, which concludes the installation phase. Then, the holding capacity of the prototype will be determined, which will indicate how much upward force the prototype can withstand. Lastly, the holding capacity of the suction caisson design will be subjected to aforementioned cyclic loading. The holding capacity is amongst others dependent on the friction between the caisson structure and the soil in which it will drive itself, therefore the composition of the soil is directly related to the ability of the suction caissons to continuously withstand cyclic loading. This research will aim to determine the critical properties multiple possible seafloor compositions have, by means of literature research. The deliverable for Ocean Grazer B.V. will then be an overview of the performance of the prototype and recommendations for future research. The Design Goal of this research is determined as follows.

Defining soil-effects on suction caisson operation based on literature analysis and experiments with regard to different compositions and conditions of ocean floor soil, such that optimal configurations for proposed suction anchor operations in different regions can be determined effectively and with relative ease.

3.2 Research Questions

To achieve the aforementioned design goal, the main question is determined as follows:
How do soil compositions and conditions of the ocean floor affect the technical feasibility of the proposed Ocean Battery suction caisson operation?

In order to answer this question, a set of sub-questions must be answered. Most importantly, it must be properly highlighted which soil properties and suction anchor properties affect the technical feasibility of suction caisson operations. As suction anchor operations includes two aforementioned phases, the sub-questions will be divided based on which phase they relate to. This leads to the following set of sub-questions:

General:

- Which criteria, parameters and conditions specifically are of importance to the successful operation of the proposed suction caisson operation?

Installation:

- To what extent does the soil composition affect the self-weight penetration of the suction caissons?
- How does soil composition affect the current design's ability to correct its rotation with respect to the ocean floor?

Operation:

- How does soil composition affect the holding capacity of the suction caisson?
- How does the soil composition affect the risks of shear failure and piping?
- How does the soil composition affect the proposed suction caisson's ability to withstand (cyclic-) loading?

4. Relevant Literature

4.1 Ocean Foundation Properties

The Ocean Foundations is 2 meters by 2 meters, with the circular suction caissons adding 74,39mm to each side. The Ocean Foundation Prototype weighs 562.7 kg whilst the Ocean Battery Prototype weighs 527.2 kg, thus the total weight of the structure is 1089,9 kg, or 10692N (Ocean Grazer, 2020). On each corner of the foundation sits a circular suction caisson with an external radius of 254 mm and an internal radius of 249 mm at the bottom, which extends upward along a length of 470 mm. Then, for the remaining 30 mm, the internal radius is gradually expanded to a radius of 253 mm. Its volume per circular caisson is 96,99 litres with a total volume of 387.94 litres for all four circular caissons. The square caisson in the middle has a volume of 72 litres, and each trapezium-shaped caisson has a volume of 139,48 litres each. Together, the square caisson and all four trapezium-shaped caissons have a volume of 629,48 litres. Figure 5 details a bottom view of the Ocean Foundation, where each of the 9 suction caissons is numbered. The sections a), b) and c), shown in Figure 5 in blue, denote the lengths of lengths of the sections that make up the rectangular caissons. These lengths are 1285.58mm, 600mm and 483.05mm for a), b) and c) respectively. The circular caissons protrude the structure by 0.3m, whilst the square caissons add another 0.2m of depth, leading to a total of 0.5m. The square caisson and the four trapezoidal-shaped caissons, denoted by numbers 5 to 9, will collectively be referred to as the rectangular caissons, as opposed to the circular caissons.

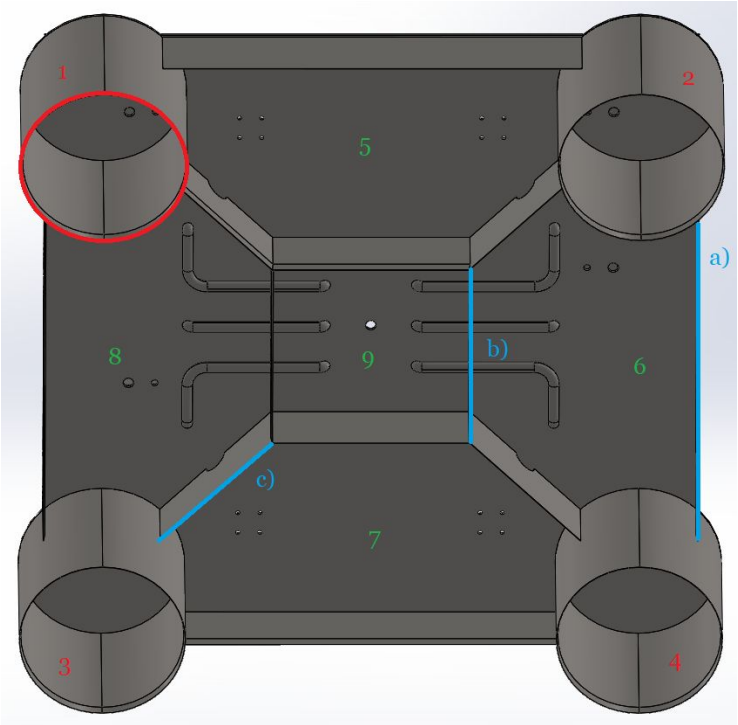

Figure 5. Overview of separate suction caisson sections (Ocean Grazer, 2020)

The concrete structure that serves as the foundation for the Ocean Battery houses a reservoir of approximately 806,3 litres, with the bladder itself adding 65,9 litres. The effective weight of the Ocean Battery once installed is decreased by the buoyancy force generated by the volume of the structure.

It is important to note that, as the Ocean Battery is in use, this constant fluctuation in effective weight will subject the suction caissons to Cyclic Loading. The properties and composition of the ocean floor will determine how resistant the suction caisson operation is against these forces, due to their effect on the holding capacity of the suction caissons (Ahn et al, 2014). The holding capacity denotes the ability of the suction caisson structure to withstand upward lift, dependent on the friction of the suction caisson with the soil, the suction force and the weight of the structure (Wang et al, 2018). The current set-up of the Ocean Battery features a 9-way suction caisson structure, with the internal caissons featuring a square- and four trapezoidal shapes whilst the corner-caissons are circular (Ocean Grazer, 2020).

The total weight of the Ocean Foundation and the Ocean Battery together is 1089,9 kg or 10691,9 N. However, the reservoirs within both structures result in an upward buoyant force, resulting in an effective unit weight of 950,9 kg or 9328,6 N. Each circular caisson then supports an estimated quarter of the total effective weight, which comes to 2332,155 N.

4.2 Local sediment

In the summer of 2020, Ocean Grazer B.V. plans to install a 1:1 scale prototype of their modular products, in the Eemshaven port (Ocean Grazer, 2020). Therefore, the scope of this research will be limited to the ocean floor compositions found in the surrounding North Sea. Due to the proximity of the North Sea, the ocean floor composition here will most likely serve as installation sites. Therefore, we will analyse the North Sea's sediment quantitatively, to determine which sediment type is most likely to be encountered, such that distinct categories may be formed for the most prominent types. The North Sea Atlas by Paramor et al. combines previous research in an effort to map the entirety of the North Sea region based on its sediment (Parabor et al, 2009). Figure 6 features a detailed map from Paramor et al., detailing different sediment types present in the North Sea.

Classifications

The International Organization for Standardization has formulated a table of standards by which soil types can be classified, based on size (ISO, 2002). These classifications will be used in this research to determine which specific soil types such as sands are present on the North Sea floor. An overview of classifications is displayed in Table 1.

Table 1: ISO Soil classifications **(ISO, 2002)**

Name	Classification	Size Range (mm)
Very coarse soil	Large Boulder	>630
	Boulder	200 - 630
	Cobble	63 - 200
Gravel	Coarse Gravel	20 - 63
	Medium Gravel	6.3 - 20
	Fine Gravel	2.0 - 6.3
Sand	Coarse Sand	0.63 - 2.0
	Medium Sand	0.2 - 0.63
	Fine Sand	0.063 - 0.2
Silt	Coarse Silt	0.02 - 0.063
	Medium Silt	0.0063 - 0.02
	Fine Silt	0.002 - 0.0063
Clay		≤0.002

Sands

From figure 6 we can conclude that the majority of the soil in the North Sea consists of fine sands. Whilst the classification in the Atlas might not be as accurate, by far the most common type of fine sand found within the North Sea is silica sand, with an average diameter between 0.83mm and 0.15mm (McLaws, 1971). Under coarse sands we could interpret coral- and biogenic sands. Biogenic sand however, is not usually found within the North Sea. Although, due to the presence of small reefs (van der Reijden et al, 2019), small pockets of coral-type sands may exist. Their presence however, will be quite minimal and will most likely be mixed with other types of sediments. Therefore, this sand type is not included within this research. Instead, Silica sand will be the primary testing sand. In their research, Li et al. and Zhang et al. use Qingdao sand for their suction caisson experiments, which they describe as a fine, dense sand (Li et al, 2015; Zhang et al, 2017).This sand will be used as well in order to study how well the Ocean Foundation fares in dense sands. In a study with regard to the pull-out capacity of suction caisson, Wachowski defined the standard properties of Silica sand which will be used in this study as it is a common marine sand (Wachowski, 2016).

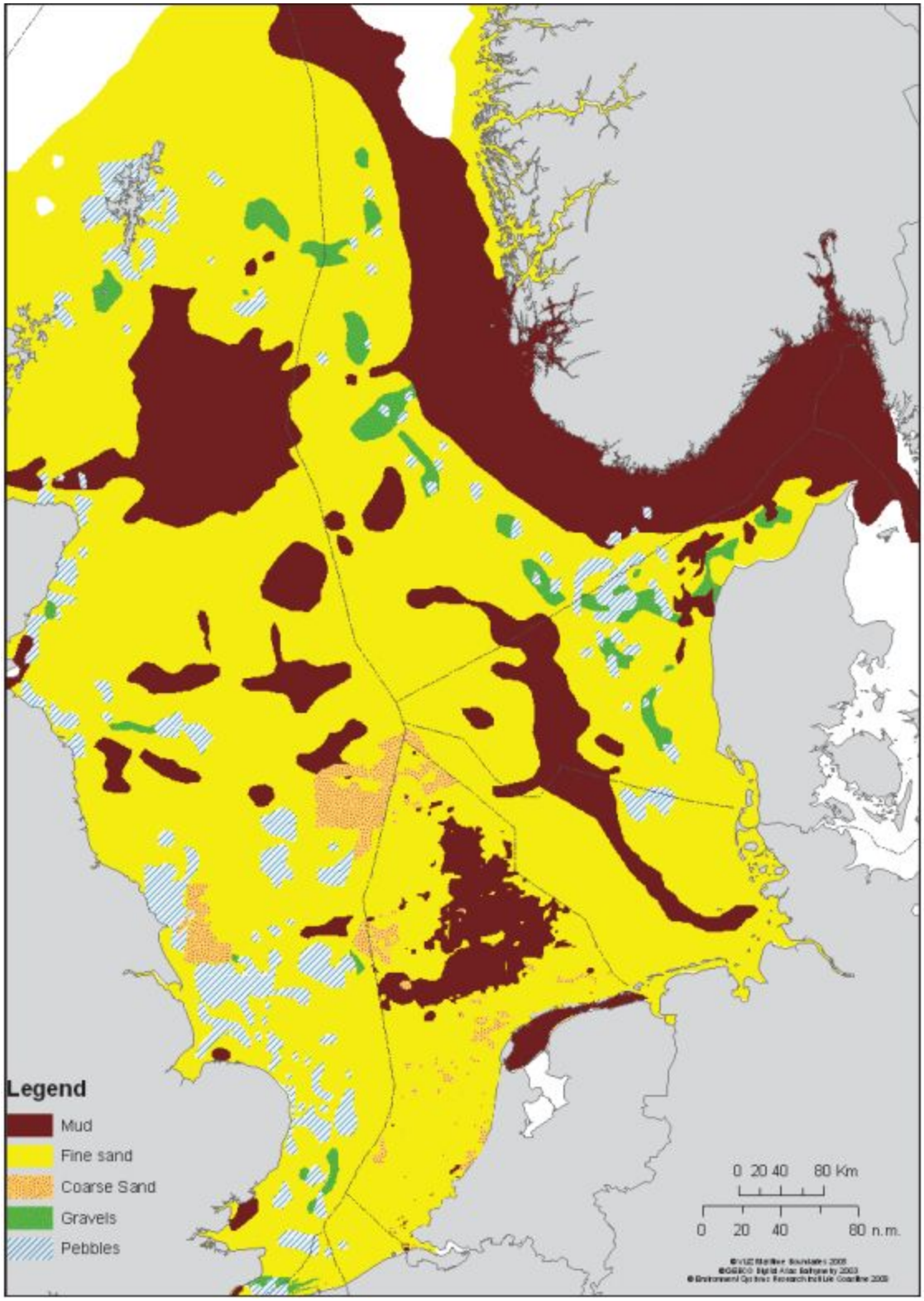

Figure 6. Detailed sediment map of the North Sea (Parabor et al, 2009)

Clays and Organic Silts

A study performed by Zhou et al. in 2006 used Kaolin Clay specifically for their experiments with regard to suction anchor operation (Zhou et al, 2006). Here, they presented justifications and further references as to why this specific clay was chosen for experiments. In this research, the aforementioned study by Zhou et al. will be used to determine which clay properties will be appropriate for the Ocean Grazer project. In order to study the Ocean Foundation's performance in cohesive soils with higher, Qiantang River silt will be used, based on a study by Wang et al. (Wang et al, 2013).

Mud and Gravels

A research by Bockelmann et al. in 2018 aimed to map the mud content and average grain sizes of areas within the North Sea (Bockelmann, 2018). However, mud is generally considered to be too liquid to properly facilitate suction caisson installation, as the high water-content leads to problems such as seepage flow, piping and shear failure. Houlsby & Byrne conclude that installation in coarse soils, such as gravels, will bring significant problems. Most prominently, the large average grain size will result in high amounts of flow during installation (Houlsby et al, 2005).

4.3 Suction Anchor Operations

In order to define which specific issues are prone to arise during suction anchor installation and operation, a multitude of studies will be included in this research. A study by Wang et al. in 2013 detailed soil failure and soil liquefaction due to suction caisson operation (Wang et al, 2013). A study by Zhang et al. in 2017 detailed the suction caisson operation in dense sand specifically, where they discussed seepage leaks amongst others (Zhang et al, 2017). Furthermore, a study by Li et al. in 2015 discussed the holding capacity of suction caissons in marine sands (Li et al, 2015). Most prominently, the study by Houlsby et al. in 2005 will be used to determine design parameters for suction caissons in different soil types (Houlsby et al, 2005).

5. Tools & Methods

This section will explore known methods of previous researches for determining aforementioned factors during suction caisson installation. As the suction caisson is lowered to the ocean floor, it is to first penetrate it through its own weight. A pump will then create an underpressure in the caisson, causing it to suck itself into the soil (Zhou et al, 2006). The main formulas that describe the behaviour of both self-weight penetration and suction-assisted penetration is described by Houlsby & Byrne (Houlsby et al, 2005). They differentiate between a method used for installation in non-cohesive soils such as sands, and a method for installation on cohesive soils such as clays and silts.

5.1 Installation - Cohesive Soils

Houlsby & Byrne defined the factor P or Penetration Resistance for cohesive soils. This factor was further used for testing of suction caisson operation in clay by Wang et al in 2018 (Wang et al, 2018). Here, they defined the term Penetration Resistance P as follows in simplified form.

$$P = W' + s\left(\frac{\pi D^2}{4}\right) \quad (1)$$

Where W' denotes the effective weight of the caisson, s denotes the suction pressure and D denotes the diameter of the caisson. This equation has been further detailed by Houlsby & Bourne to include 3 separate terms that denote the frictional resistance between the soil and the outer surface, inner surface, and the resistance due to the thickness of the caisson, respectively (Houlsby et al, 2005). The relation is described as follows:

$$W' = h\alpha_0 s_{u1}(\pi D_0) + h\alpha_i s_{u1}(\pi D_i) + (\gamma' h N_q + s_{u2} N_c)(\pi D t) \quad (2)$$

Where h denotes the installed depth of the caisson, α_o and α_i denote the adhesion factor of the inside and outside of the caisson respectively. Additionally, s_{uo}, s_{u1} and s_{u2} denote the shear strength at the mudline, average shear strength over depth of skirt, and shear strength at the caisson skirt tip respectively. Furthermore, D_o and D_i denote the outside and inside diameters of the caisson, where D now denotes the mean diameter. Lastly, γ' denotes the effective unit weight of the soil, N_c denotes the cohesion bearing capacity factor, N_q denotes the overburden bearing capacity factor and t denotes the wall thickness. Note that the effective unit weight is defined as the unit weight γ of the soil minus the unit weight of water γ_w, where γ_w is equal to 9,807 kN/m^3. Wang et al. combined these equations as follows to describe suction-assisted penetration.

$$P = W' + s\left(\frac{\pi D^2}{4}\right) = h\alpha_0 s_{u1}(\pi D_0) + h\alpha_i s_{u1}(\pi D_i) + (\gamma' h - s + s_{u2} N_c)(\pi D t) \quad (3)$$

Note that here, s_{u1} and s_{u2} are defined as follows:

$$s_{u1} = s_{u0} + \rho\frac{h}{2} \tag{4}$$

$$s_{u2} = s_{u0} + \rho h \tag{5}$$

Here, s_{uo} is the shear strength at the mudline and ρ denotes the rate of change of the shear strength with depth. Due to the inherent uncertainty within soil mechanics, Chen defined a range of values for ρ in multiple kaolin clays, which can be collected in an average rate of change (Chen, 2007).

The suction term s is limited by the difference between the inside- and outside stress at the tip of the caisson. If the difference becomes too great, a 'reverse' bearing capacity problem will occur, where soil flows inward. The condition at which this problem arises is described by Houlsby & Byrne as follows (Houlsby et al, 2005).

$$-s + \gamma' h + \left(\frac{\pi D_i h \alpha_i s_{u1}}{\pi D_i^2/4}\right) = \gamma' h + \left(\frac{\pi D_0 h \alpha_0 s_{u1}}{\pi(D^2 - D_0^2)/4}\right) - N_c^* s_{u2} \tag{6}$$

Where N_c* is a BCF appropriate for uplift of a buried circular footing.

5.2 Installation - Non-cohesive soils

Houlsby & Byrne defined a relation for non-cohesive soils such as sands, similar to equation 2. This relation is given by equation 7 (Houlsby et al, 2005). This relation was previously described by K. van der Loo in his research with regard to the Ocean Grazer project as well (K. van der Loo, 2020).

$$W' = \frac{\gamma' h^2}{2} K \tan(\delta)_0 (\pi D_0) + \frac{\gamma' h^2}{2} K \tan(\delta)_i (\pi D_i) + (\gamma' h N_q + \gamma' \frac{t}{2} N_\gamma)(\pi D t) \tag{7}$$

Here, K is the vertical to horizontal stress factor and δ is the interface friction angle. Additionally, N_q is the aforementioned bearing capacity factor, and N_γ is the self-weight bearing capacity factor. As with equation 2, this equation too is divided in three terms which each describe the friction on the outside, inside and on the caisson tips respectively. This equation however is simplified according to Houlsby & Byrne, as it does not take into account the enhancement of vertical stress close to the pile, which are caused by frictional forces further up the caisson. Thus, Houlsby & Byrne present a modified equation which does take these forces into account, shown in equation 8.

$$\begin{aligned} W' = {} & \gamma' Z_0^2 (\exp(\tfrac{h}{Z_0}) - 1 - (\tfrac{h}{Z_0}))(K \tan(\delta)_0 (\pi D_0) \\ & + \gamma' Z_i^2 (\exp(\tfrac{h}{Z_i}) - 1 - (\tfrac{h}{Z_i}))(K \tan(\delta)_i (\pi D_i) + \sigma'_{end} (\pi D t) \end{aligned} \tag{8}$$

Here, Z_o and Z_i are defined as follows:

$$Z_0 = \frac{D_0(m^2-1)}{(4(K\tan(\delta))_0} \quad (9)$$

$$Z_i = \frac{D_i}{(4(K\tan(\delta))_i} \quad (10)$$

Where m is a constant with a relation to the outer diameter D_o.
The variable σ'_{end} is a collective effective stress term which depends on the variables σ'_{vo} and σ'_{vi}, which denote the outside- and inside effective vertical stress respectively. Their overall relation is dependent on an inequality, which leads to the following equations for σ'_{end}.

$$\sigma'_{end} = \sigma'_{v0}N_q + \gamma'(t - \frac{2x^2}{t})N_\gamma \quad (11)$$

$$\text{If } \sigma'_{vi} - \sigma'_{v0} < \frac{2t\,N_\gamma}{N_q}\text{, then} \qquad x = \frac{t}{2} + \frac{(\sigma'_{v0} - \sigma'_{vi})N_q}{4\gamma' N_\gamma} \quad (12)$$

$$\text{If } \sigma'_{vi} - \sigma'_{v0} \geq \frac{2t\,N_\gamma}{N_q}\text{, then} \qquad x = 0 \quad (13)$$

The values of σ'_{vo} and σ'_{vi} are calculated as follows.

$$\sigma'_{v0} = \gamma' Z_0\,(\exp(\frac{h}{Z_0}) - 1) \quad (14)$$

$$\sigma'_{vi} = \gamma' Z_i\,(\exp(\frac{h}{Z_i}) - 1) \quad (15)$$

For suction-assisted penetration, Houlsby and Byrne suggest the following equation.

$$\begin{aligned} W' + s(A_i) = {} & (\gamma' + \frac{as}{h})Z_0^2(\exp(\frac{h}{Z_0}) - 1 - (\frac{h}{Z_0}))(K\tan(\delta))_0(\pi D_0) + \\ & (\gamma' - \frac{(1-a)s}{h})Z_i^2(\exp(\frac{h}{Z_i}) - 1 - \frac{h}{Z_i}))(K\tan(\delta))_i(\pi D_i) + \\ & (\gamma' - \frac{(1-a)s}{h})Z_i(\exp(\frac{h}{Z_i}) - 1)N_q + \gamma' t N_\gamma)(\pi D t) \end{aligned} \quad (16)$$

Where A_i is the inside area of the caisson and a is defined as follows.

$$a = \frac{a_1 k_f}{(1-a_1)+a_1 k_f} \quad (17)$$

Here, k_f is the ratio between inside- and outside permeability, for which Houlsby and Byrne propose a value of $k_f = 1$. (Houlsby et al, 2005). Furthermore, a_1 is defined as follows.

$$a_1 = c_0 - c_1(1 - \exp(-\frac{h}{c_2 D})) \quad (18)$$

Here, the values of c_i are proposed by Houlsby and Byrne as well, namely: c_o = 0.45; c_1 = 0.36 and c_2 = 0.48 (Houlsby et al, 2005).

According to Houlsby & Byrne, the issue of piping can arise if the suction forces are too great, which prevents further installation. The condition for piping is described as follows.

$$s = \frac{\gamma' h}{(1 - a)} \tag{19}$$

If the suction term s on the left hand side becomes greater than the term on the right hand side, piping will prevent further installation of the caisson (Houlsby et al, 2005).

5.3 Bearing Capacity Factors

The cohesion bearing capacity factor N_c is dependent on the effective internal angle of friction of the soil, denoted by φ'. If φ' is equal to 0, N_c is equal to 5.14 (Terzaghi, 1943), however if φ' is larger than 0, N_c is defined as follows.

$$N_c = \frac{N_q - 1}{\tan(\varphi')} \tag{20}$$

In turn, N_q is defined as follows.

$$N_q = \frac{e^{2\pi(0.75 - \varphi'/360)\tan(\varphi')}}{2\cos^2(45 + \varphi'/2)} \tag{21}$$

The self-weight bearing capacity factor N_γ is dependent on a constant $K_{p\gamma}$. Terzaghi finds the value of this constant graphically using a tedious method, however D.P. Coduto found a way to define N_γ that does not rely on $K_{p\gamma}$ using an approximation method (Coduto, 2001). Coduto's definition of N_γ is found below.

$$N_\gamma = \frac{2(N_q + 1)\tan(\varphi')}{1 + 0.4\sin(4\varphi')} \tag{22}$$

All the aforementioned equations rely either directly or indirectly on soil properties. Therefore, they can be used to derive theoretical values of suction caisson parameters which can then be used for comparison, in turn leading to the formulation of distinctive categories for different soil types.

5.4 Holding Capacity - Cohesive soils

The holding capacity or uplift capacity in cohesive soils, such as clays, is difficult to determine. As such, most studies incorporate either experiments or simulations in an effort to determine the holding capacity of suction anchors. Studies by Villalobos et al. and Chen et al. detail aforementioned experiments, whilst a study such as the one performed by Zhou et al. details how the holding capacity was approximated using Finite Element Analysis or FEA (Villalobos et al, 2010; Chen, 2007; Zhou et al, 2006). While determining the holding capacity of suction

caissons in cohesive soils analytically is difficult, there are other methods to approximate its value. Jostad et al. use numerous formulas that are usually applied in pile foundation design, however their approach relies on various assumptions that may not be applicable in this research (Jostad et al, 2015).

In their study, Iskander et al. state that the undrained pullout capacity of a circular caisson can be defined as the sum of all downward forces including weight and friction (Iskander et al, 2011). They define the undrained pullout capacity Q as follows.

$$Q = Q_{so} + Q_b + W_c + W_s \tag{23}$$

Here, Q_{so} is the side shear stress on the outside wall of the caisson, Q_b is the tensile bearing capacity of the foundation soil, W_c is the submerged weight of the caisson and W_s is the submerged weight of the soil plug. The variables Q_{so} and Q_b are calculated as follows in cohesive soils.

$$Q_{so} = \int_0^H \alpha s_{u0} \pi D_0 dh \tag{24}$$

$$Q_b = s_{u0} N_c f(\tfrac{\pi}{4}) D_0^2 \tag{25}$$

Where H is the depth of the tip of the caisson, α is a friction factor which is taken as the aforementioned adhesion factor and f is a bearing capacity correction coefficient. While no clear value of f is proposed, through reproduction of the experiments in the study by Iskander et al., a value for $f \approx 0.7$ can be determined (Iskander et al, 2011). A value of 9 will be used for the cohesion BCF N_c, as is recommended by Iskanker et al. The holding capacity of the entire system would then be described as the sum of the holding capacity of all four circular caissons, the holding capacity of the larger, rectangular caisson, the weight of the caisson and the sum of the weights of the soil plugs in each circular caisson and the rectangular caisson.

These formulas pose one issue, namely the fact they are designed for circular caissons rather than rectangular caissons. Therefore, the outer diameter D_o in equations 24 and 25 will be replaced with the length of the diagonal D_r, which is shown graphically in figure 7. As mentioned earlier, by design the five separate rectangular suction caisson chambers will act as one, therefore the assumption is made that it consists of one chamber as a whole. The length D_r is then 2320.43mm.

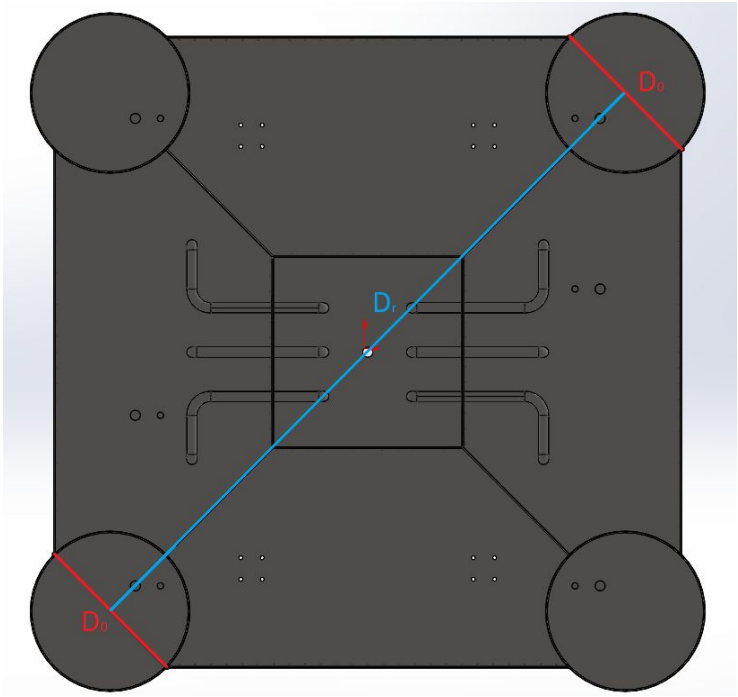

Figure 7. Visual representation of the length D_r through the circular caisson outer diameter D_o.

5.5 Holding Capacity - Non-cohesive soils

The holding capacity for non-cohesive soils, such as sands, is likewise usually determined through either simulations or physical experiments. In their study, Hung et al. describes an equation that can be used to calculate the theoretical value of the holding capacity in sands (Hung et al, 2017). Similar to the approach for cohesive soils, the holding capacity is given to be a sum of the stress on the outside and inside of the caisson. This approach was used as well by van der Loo in his study for the previous Ocean Foundation prototype (van der Loo, 2020). The equation is given as follows.

$$H_c = R_{s(OS)} + R_{s(IS)} \tag{26}$$

Where H_c is the holding capacity of the system and $R_{s(OS)}$ and $R_{s(IS)}$ are the frictional resistance between the soil and the outer- and inner caisson skirt respectively. These resistance forces are in turn calculated as follows.

$$R_{s(OS)} = R_{s(IS)} = \frac{\gamma' h}{2} K \tan(\delta) \pi D h \tag{27}$$

It should be noted that equation 26 as given by Hung et al. does not include the weight of the foundation W_c, nor the weight of the soil plug W_s, as seen in the previous section for cohesive soils. The study by Iskander et al. shows that for sands, these weights increase the holding capacity of the system (Iskander et al, 2011). Therefore, equation 26 can be modified as follows to include the weight of the caisson and the weight of the soil plug.

$$H_c = R_{s(OS)} + R_{s(IS)} + W_c + W_s \tag{28}$$

Equation 27 will have to be modified as well so that it may be used to calculate the holding capacity of the aforementioned rectangular caissons. The diagonal length D_r will be used as mean diameter D, similar to the method for cohesive soils. The diagonal D_r is displayed visually in figure 7.

6. Data Acquisition

6.1 Cohesive Soils

In their study, Wang et al., suggests an adhesion factor of 0.35 for both the outside- and inside adhesion factor, α_o and α_i respectively for the soft clay that they use (Wang et al, 2018). Wang et al. states that the adhesion factor is given by the inverse of the soil sensitivity. The soil sensitivity is a ratio that describes how well the shear strength of the soil is preserved after the soil has been remoulded, i.e. through the application of force (Abuhajar et al, 2010). Houlsby & Byrne define multiple possible values for the adhesion factor for standard clays, namely 0.45, 0.50 or 0.60, though the latter is only used for the outside adhesion factor (Houlsby & Byrne, 2005). In this research, it is assumed that the adhesion factor for both the Kaolin clay and the Qiantang River silt is 0.50 as they share a similar average grain size.

In their study, Suzuki defined the effective internal angle of friction for Kaolin clay to be 23.4° with a cohesion of 12.8 kPa (Suzuki, 2017).

Table 2: Rate of change of shear strength ρ as defined by Chen for multiple different clays (Chen, 2007)

Clay type	Test number	ds_u/dz (kPa/m)
NC	B12sus	1.23
	B12SCC	1.17
LOC	B13sus	1.76
	B13SCC	1.64
Sensitive	B14sus	1.33
	B14SCC	1.16
Sensitive	B14susa	1.58
	B14SCCa	1.58

In their research, Zhou et al. determined the undrained shear strength and rate of change for the shear strengths for Kaolin clay. Here, he described s_{uo} = 4 + 1.5h kPa, thus equalling the rate of change ρ to 1.5 kPa/, and s_{uo} = 4 kPa. (Zhou et al, 2006). In the study by Chen in 2007, he defined a range of rates of change, which are shown in Table 2 (Chen, 2007).

From Table 2 an average rate of change can be calculated, which gives ρ = 1.431 kPa/m, which is quite close to the rate of change reported by Zhou et al of ρ = 1.5 kPa/m. As the shear strength of a soil is partly dependent on its cohesion, it can reasonably be assumed that the higher value of cohesion for the Kaolin clay results in a larger rate of change as opposed to the Qiantang River silt. Therefore, the following assumption is made for the Kaolin clay: ρ = 1.45 kPa/m, and for the Qiantang River silt: ρ = 1.35 kPa/m. Due to the lack of further reference, the undrained shear strength of the Qiantang River silt must be estimated. In their study, Sun et al. approximated the drained shear strength of silt under various stress circumstances in unsaturated conditions (Sun

et al, 2007). Combining this study with available parameters from the study by Wang et al., the value of s_{uo} for the clayey Qiantang River silt is estimated to be s_{uo} = 6 kPa.

The classifications used by the Unified Soil Classification System (USCS), can be used to validate the values chosen for the cohesion and the internal angle of friction. The classifications are displayed in Table 3 (USCS, 2017). The Kaolin clay that is studied in this research would be an organic clay, whilst the Qiantang River silt studied in this research would be a silt or organic silt. The USCS shows that the assumptions made for this research are fairly accurate, the most notable difference being the 0 kPa cohesion noted for standard silts. The Qiantang River silt however is described to be fairly clayey, therefore the assumptions made are fairly accurate as well (Wang, 2013).

6.2 Non-cohesive Soils

In a similar manner, the properties of the sands used in this study can be determined and if necessary, approximated. Houlsby & Byrne give a value of 0.63 for $K\tan(\delta)$, for a sand with similar properties to the sands that will be studied in this research. Due to the complexity of finding the value of $K\tan(\delta)$, this given value will be used. The value of m in this research will be taken as 1.4, as given by Houlsby & Byrne as well (Houlsby et al, 2005).

In his study, Wachowski defined the dry unit weight of silica sand. By subtracting the unit weight of water, the effective unit weight can be determined, which results in γ' = 5.993 kN/m^3 (Wachowski, 2016). Similarly, a median diameter of D_{50} = 0.20mm can be determined. Lastly, with the use of table 3, the effective internal angle of friction for Silica sand is determined to be φ' = 36° (USCS, 2017).

Most of the properties of Qingdao sand can be collected from a study by Zhang et al. and Li et al., in which they performed experiments regarding the installation and extraction of suction caissons in dense sand, in this case, Qingdao sand (Zhang et al, 2017; Li et al, 2015). Here, they give the unit weight of Qingdao sand to be γ' = 10.2 kN/m^3. The median diameter of the sand grains in Qingdao sand, D_{50}, is given as 0.1002mm, which is notably smaller than the median diameter of grains in Silica sand. Therefore it can be concluded that Qingdao sand is indeed much denser than Silica sand. While the effective internal angle of friction is not explicitly stated, an assumption can be made through the use of table 3. Consequently, the value of φ' for Qingdao sand is estimated to be 34°, as it is a very fine sand (USCS, 2017).

Table 3: USCS Soil Classifications (USCS, 2017)

USCS Soil-class	Description	Cohesion (kPa)	Friction angle (°)
GW	well-graded gravel, fine to coarse gravel	0	40
GP	poorly graded gravel	0	38
GM	silty gravel	0	36
GC	clayey gravel	0	34
GM-GL	silty gravel	0	35
GC-CL	clayey gravel with many fines	3	29
SW	well-graded sand, fine to coarse sand	0	38
SP	poorly graded sand	0	36
SM	silty sand	0	34
SC	clayey sand	0	32
SM-SL	silty sand with many fines	0	34
SC-CL	clayey sand with many fines	5	28
ML	silt	0	33
CL	clay of low plasticity, lean clay	20	27
CH	clay of high plasticity, fat clay	25	22
OL	organic silt, organic clay	10	25
OH	organic clay, organic silt	10	22
MH	silt of high plasticity, elastic silt	5	24

7. Results

7.1 Installation - Cohesive Soils

Table 4 displays the properties of Kaolin clay and Qiantang River silt that will be used to calculate the initial penetration depth of the Ocean Foundation and Ocean Battery prototype, using equation 2. As mentioned in section 6, the Effective Weight that each circular caisson will support is 2332,155 N. This value can be used to find the initial penetration depth in each cohesive soil. Table 5 displays the properties of the circular caissons necessary to use equation 2. The BCFs can be calculated using the effective internal angle of friction that has been found. These factors are displayed in table 6.

Table 4. Properties of Kaolin clay and Qiantang River silt

Description	***Symbol***	***Unit***	***Kaolin Clay Properties***	***Qiantang River Silt Properties***
Median Diameter	D_{50}	mm	0.03	0.029
Outside AF	α_o	-	0.5	0.5
Inside AF	α_i	-	0.5	0.5
Shear Strength at mudline	s_{uo}	kPa	4	6
Rate of change *su*	ρ	kPa/m	1.45	1.35
Effective Unit Weight	γ'	kN/m^3	7.17	8.823
Effective Internal Angle of Friction	φ'	°	23.4	36.5
Cohesion	c	kPa	12.8	9.2

Table 5. Properties of the circular caissons

Description	***Symbol***	***Unit***	***Circular Caisson Properties***
Effective Weight - 1/4	W'	N	2332,155
Diameter - Outside	D_o	m	0.508
Diameter - Inside	D_i	m	0.498
Radius - Outside	r_o	m	0.254
Radius - Inside	r_i	m	0.249
Diameter - Mean	D	m	0.503
Thickness	t	m	0.005
Inside Area	A_i	m^2	0.195

Table 6. Calculated Bearing Capacity Factors for cohesive soils

Description	***Symbol***	***Unit***	***Kaolin Clay Properties***	***Qiantang River Silt Properties***
Cohesion BCF	N_c	-	22.3743	66.6946
Overburden BCF	N_q	-	10.6822	50.3514
Self-Weight BCP	N_γ	-	7.2260	62.1047

Houlsby & Byrne state that the BCF N_c* is usually described by the relation (N_c*/4α_o = 3), thus equating N_c* in this study to a value of 6 (Houlsby et al, 2005). This value will later be used in equation 6 to determine whether plastic failure will occur due to the reverse bearing capacity problem.

By using equation 2, we find the maximum self-weight penetration depth of the suction caissons for both soils. The maximum self-weight penetration depth h in Kaolin clay is 0.219 m. Interestingly, the weight of the caisson is not enough to penetrate the Qiantang River silt, as the friction forces are too high. The friction forces can be modeled as the depth h increases, which is shown in figure 8 and figure 9 for Kaolin clay and Qiantang River silt respectively.

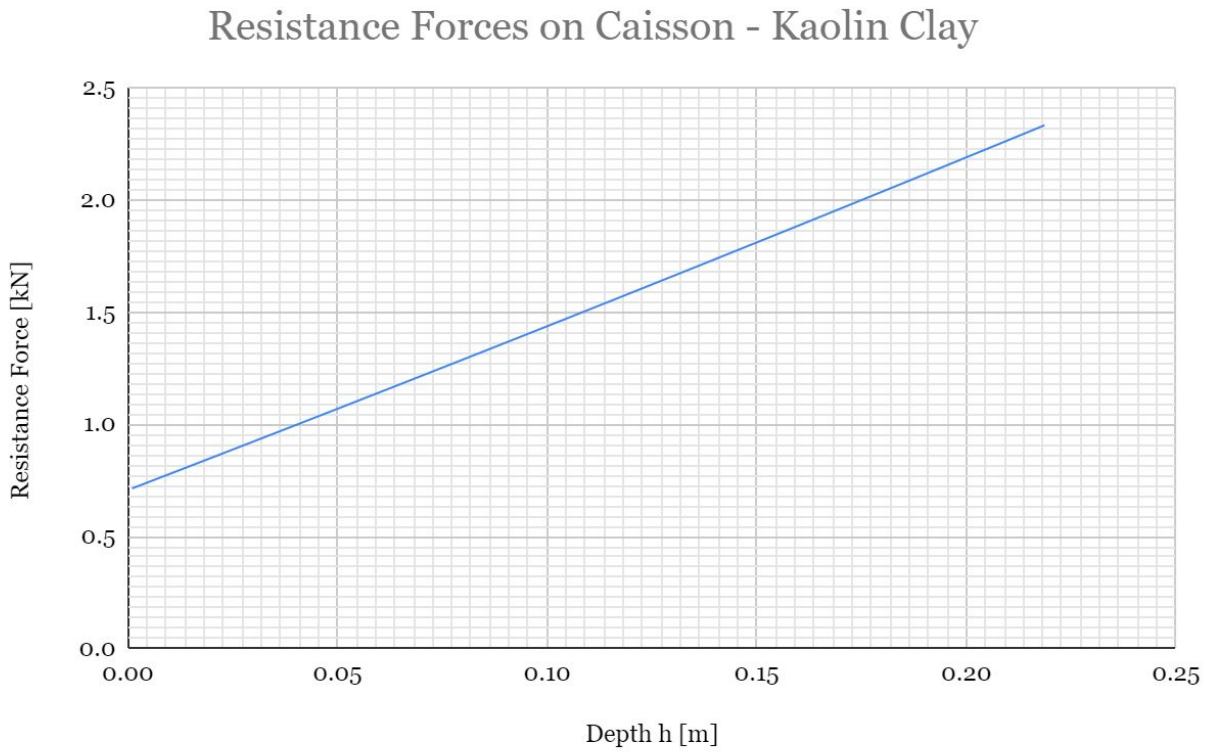

Figure 8. Frictional Forces over depth for self-weight installation in Kaolin clay

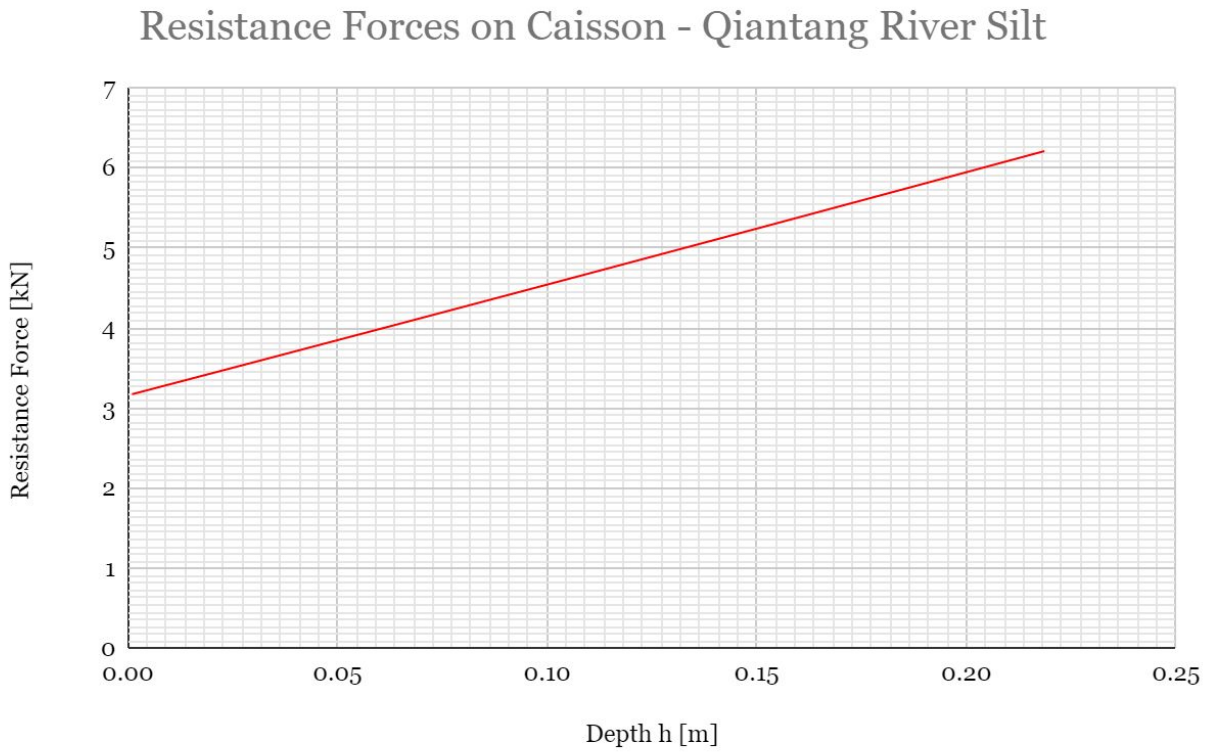

Figure 9. Frictional Forces over depth for self-weight installation in Qiantang River silt

The self weight installation depth in Kaolin clay is 0.219m of the total length of 0.5m. In Qiantang River silt, the friction forces are too great for the Ocean Grazer to penetrate using only its own weight. Equation 3 can now be used to calculate how much suction force is required for the caisson to penetrate the soil up to the maximum 0.5m. These suction forces are plotted in figure 10 for Kaolin clay and figure 11 for Qiantang River silt.

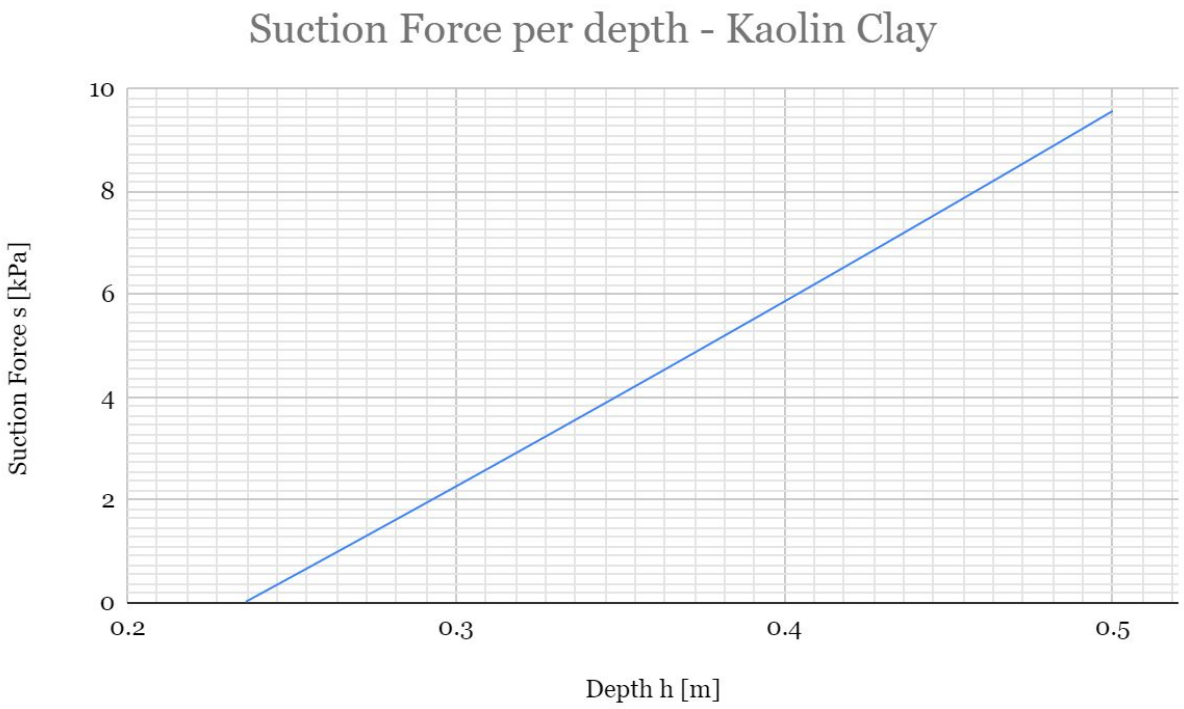

Figure 10. Required Suction Force s to reach a specific depth in Kaolin clay

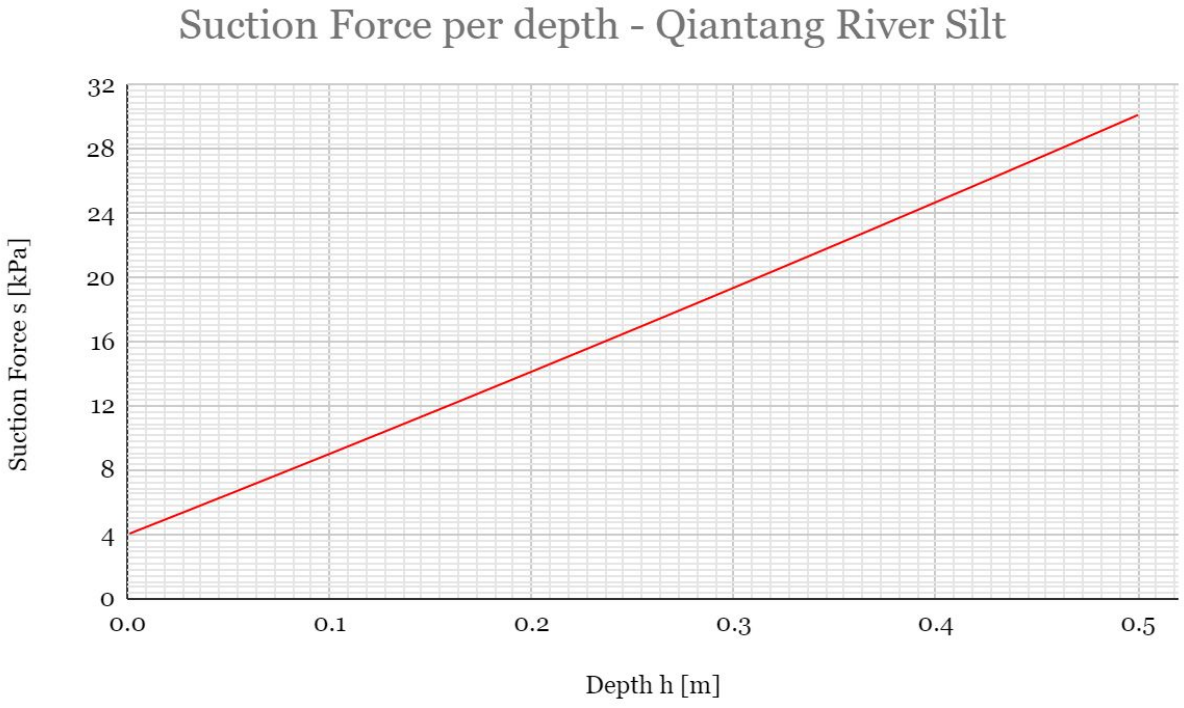

Figure 11. Required Suction Force s to reach a specific depth in Qiantang River silt

To reach an installation depth of 0.5m, a total Suction Force of 9.57 kN is necessary for Kaolin clay and 30.14 kN for Qiantang River silt. From figure 10 and figure 11 it can be concluded that an installation in Qiantang River silt requires significantly more suction force. Equation 6 shows that the inside stress in neither soil outweighs the outer stress, thus the reverse bearing capacity problem does not occur.

7.2 Installation - Non-cohesive Soils

Table 7 displays the properties of the non-cohesive soils that will be used in this study, which will be used together with the properties of the caissons displayed in table 5. Table 8 then displays the BCFs of these soils.

Table 7. Properties of Silica sand and Qingdao sand

Description	***Symbol***	***Unit***	***Silica Sand Properties***	***Qingdao Sand Properties***
Median Diameter	D_{50}	mm	0.322	0.1002
Outer Z term	Z_o	-	0.194	0.194
Inner Z term	Z_i	-	0.198	0.198
Ratio inside/outer Permeability	kf	-	1	1
K tan(δ)	$K\tan(\delta)$	-	0.63	0.63
Constant m	m	-	1.4	1.4
Effective Unit Weight	γ'	kN/m^3	5.993	10.2
Effective Internal Angle of Friction	φ'	^{o}	36	34
Constant c0	c_o	-	0.45	0.45
Constant c1	c_1	-	0.36	0.36
Constant c2	c_2	-	0.48	0.48

Table 8. Calculated Bearing Capacity Factors for non-cohesive soils

Description	***Symbol***	***Unit***	***Kaolin Clay Properties***	***Qiantang River Silt Properties***
Cohesion BCF	N_c	-	63.5283	52.6374
Overburden BCF	N_q	-	47.1560	36.5044
Self-Weight BCP	N_γ	-	56.6545	39.5927

The effective weight of the Prototype will again be taken as 2332.155 N. These properties can now be used to determine the self-weight penetration depth of the Ocean Grazer in both Silica

sand and Qingdao sand. By using equation 7, the initial penetration depths for both types of sand can be found. The self-weight penetration depth h is 0.288m for Silica sand and 0.240m for Qingdao sand. The friction forces can be displayed with regard to the installation depth, which is shown in figure 12 and figure 13 for Silica sand and Qingdao sand respectively.

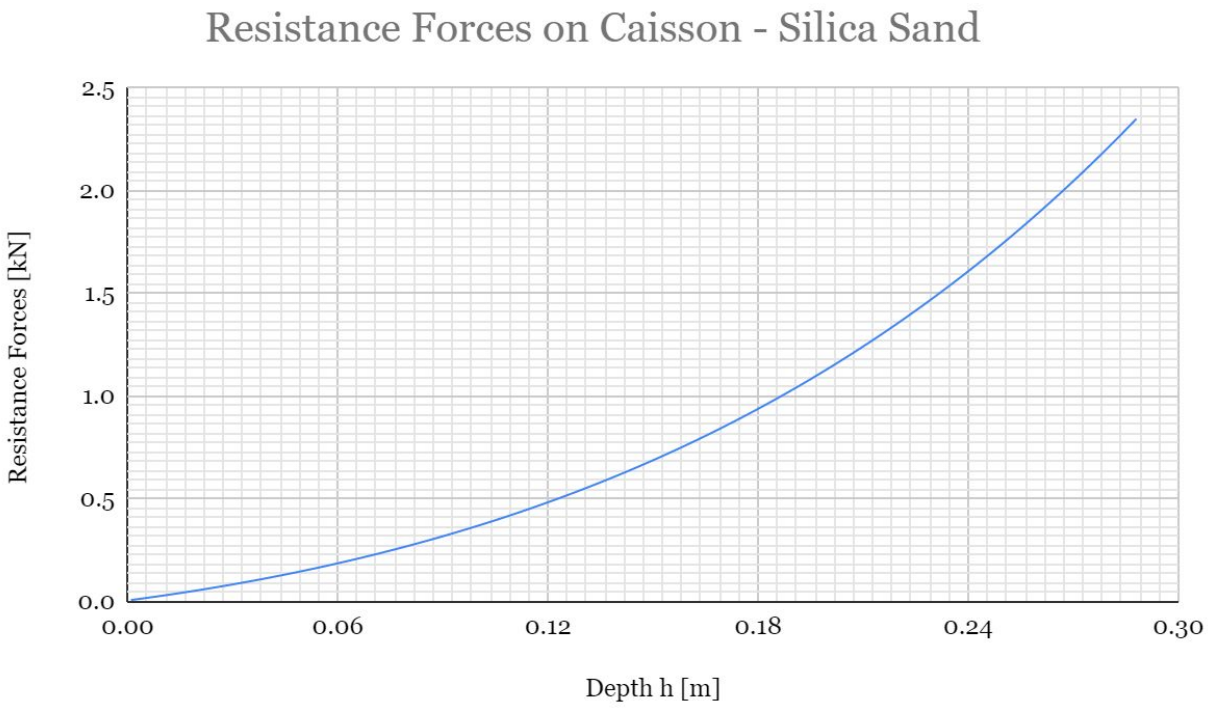

Figure 12. Frictional Forces over depth for self-weight installation in Silica sand

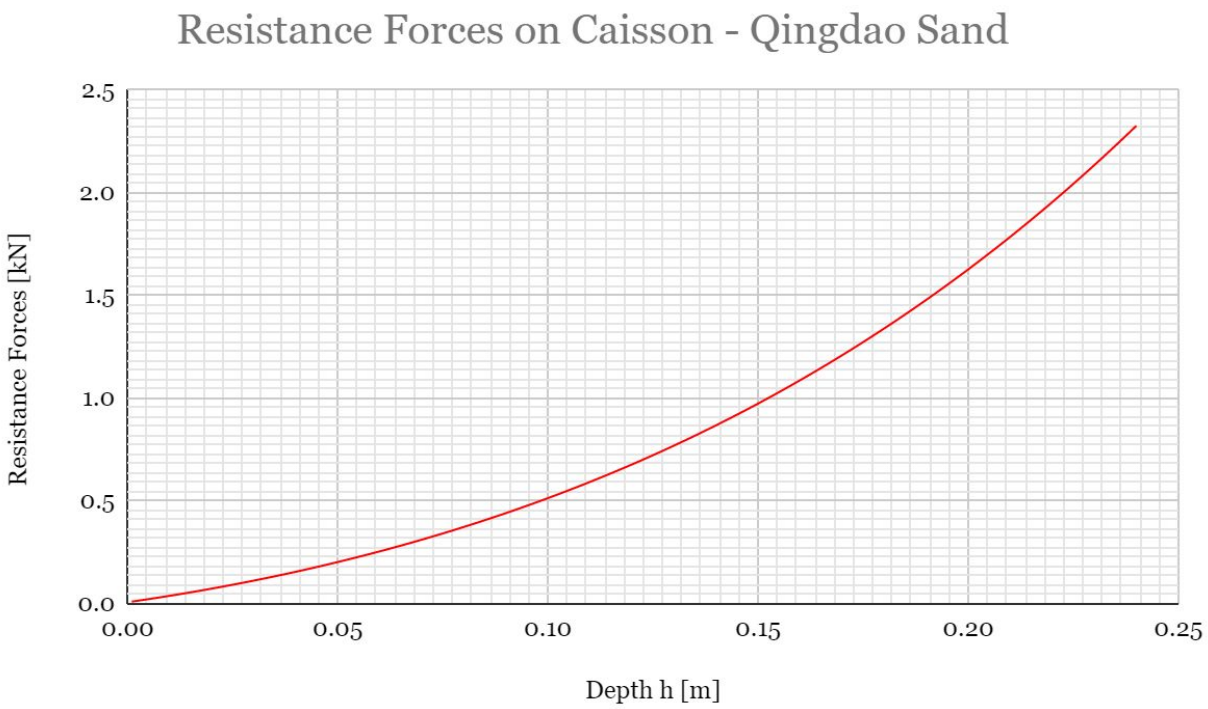

Figure 13. Frictional Forces over depth for self-weight installation in Qingdao sand

Equation 16 can now be used to display the required suction force in order for the caissons to reach the total skirt depth of 0.5m. These suction forces for Silica sand and Qingdao sand are shown in figure 14 and figure 15 respectively.

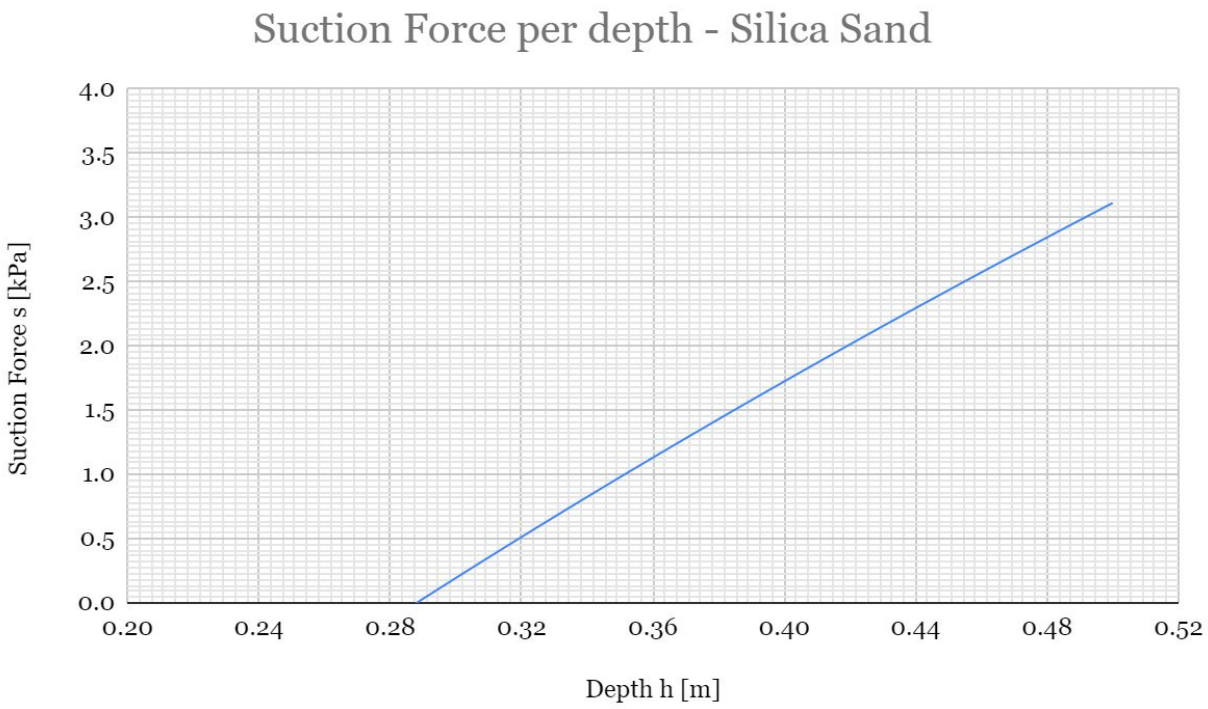

Figure 14. Required Suction Force s to reach a specific depth in Silica sand

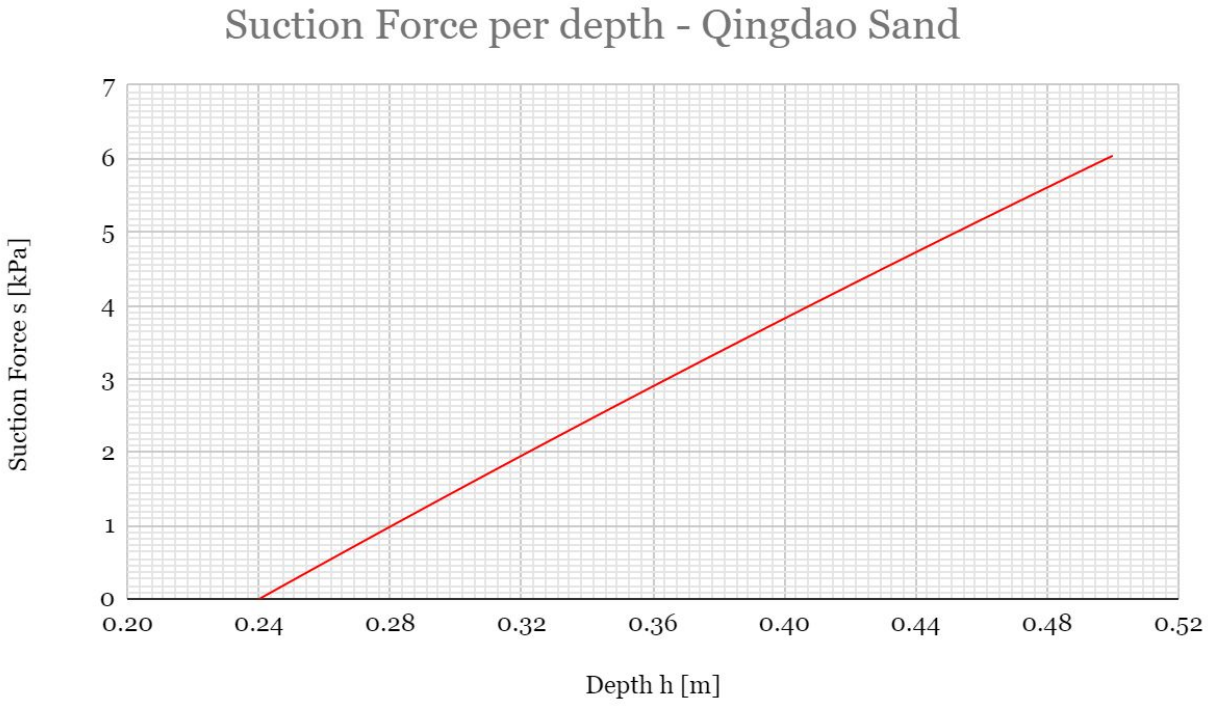

Figure 15. Required Suction Force s to reach a specific depth in Qingdao sand

In Silica sand, a suction force of 3.11 kPa is necessary to reach a depth of 0.5m. For Qingdao sand, 6.04 kPa is required. As expected, the resistance in the more dense Qingdao sand is higher than that of the Silica sand. Consequently, a higher suction force is required to reach the skirt depth in Qingdao sand as opposed to Silica sand.

With equation 19, it can be concluded that piping will not occur during installation in Silica sand. In the denser Qingdao sand however, the condition is met at a depth of h = 0.488m due to the high suction force required at that depth, meaning that piping will prevent installation over the last 1.2cm.

7.3 Rotational Correction

The effect of the suction force on how deep the caissons will install themselves can be converted to represent an angle with respect to the Prototype's centre plane instead. This can be used to determine the maximum angle to which each caisson can correct itself, in order to make the caisson as a whole levelled. The circular caissons feature an independent pump with which they can generate individual suction forces, contrary to the trapezoidal caissons located in the middle which act primarily to increase the prototype's holding capacity. Therefore, the circular caissons, with a protruding skirt length of 0.5m, are mainly responsible for correcting the Ocean Foundation's rotation if it lands slanted on the ocean floor.

The distance between the centre of the Ocean Foundation and the center of one of the four circular caissons is estimated to be 1.16021m (Ocean Grazer, 2020). That means that with a total opposing length of 0.5m, a total angle of 23.324° can be corrected. However, the self-weight installation depth needs to be subtracted from this 0.5m in order to properly define how great of an angle can be corrected. Furthermore, the suction forces required to correct up to a certain angle can be modelled for each of the soils.

The maximum angle that can be corrected in each type of soil is shown in table 9. The suction force required to correct a certain angle is visualized in figure 17, figure 17, figure 18 and figure 19 for Kaolin clay, Qiantang River silt, Silica sand and Qingdao sand respectively.

Table 9. Maximum angle that can be corrected by circular caissons in different soils

Soil	Value	Unit
Kaolin clay	13.615	°
Qiantang River silt	23.272	°
Silica sand	10.403	°
Qingdao sand	12.631	°

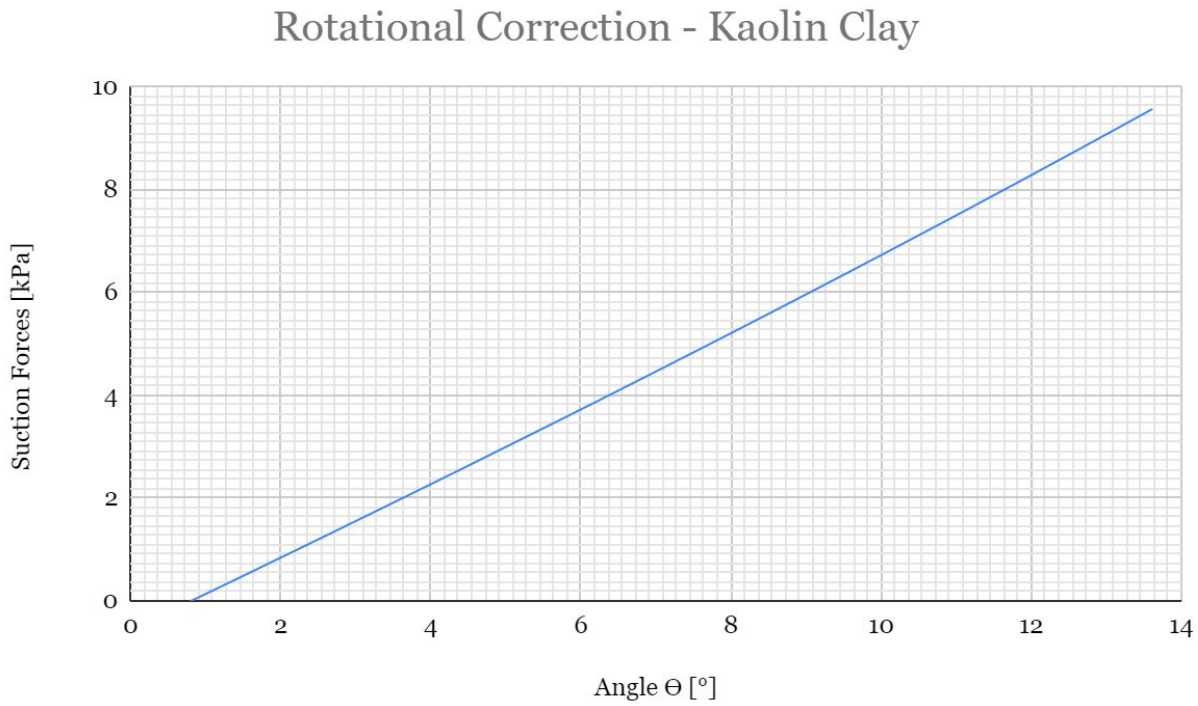

Figure 16. Required Suction Force s to correct a specific angle in Kaolin clay.

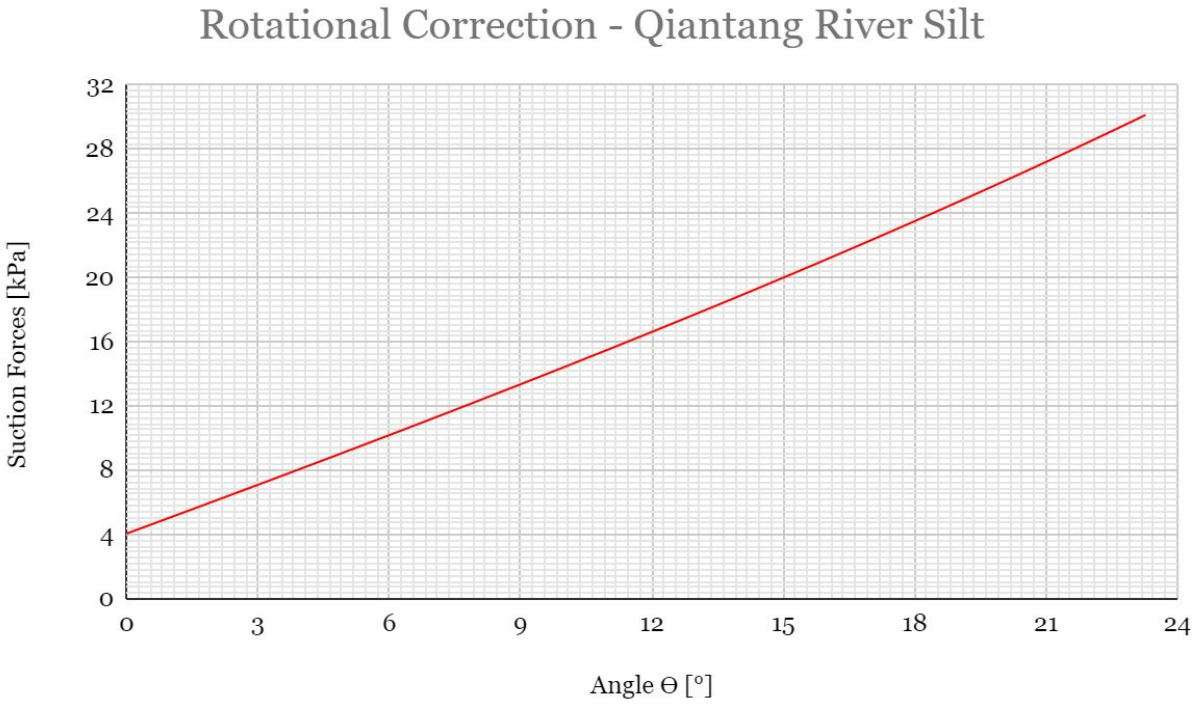

Figure 17. Required Suction Force s to correct a specific angle in Qiantang River silt.

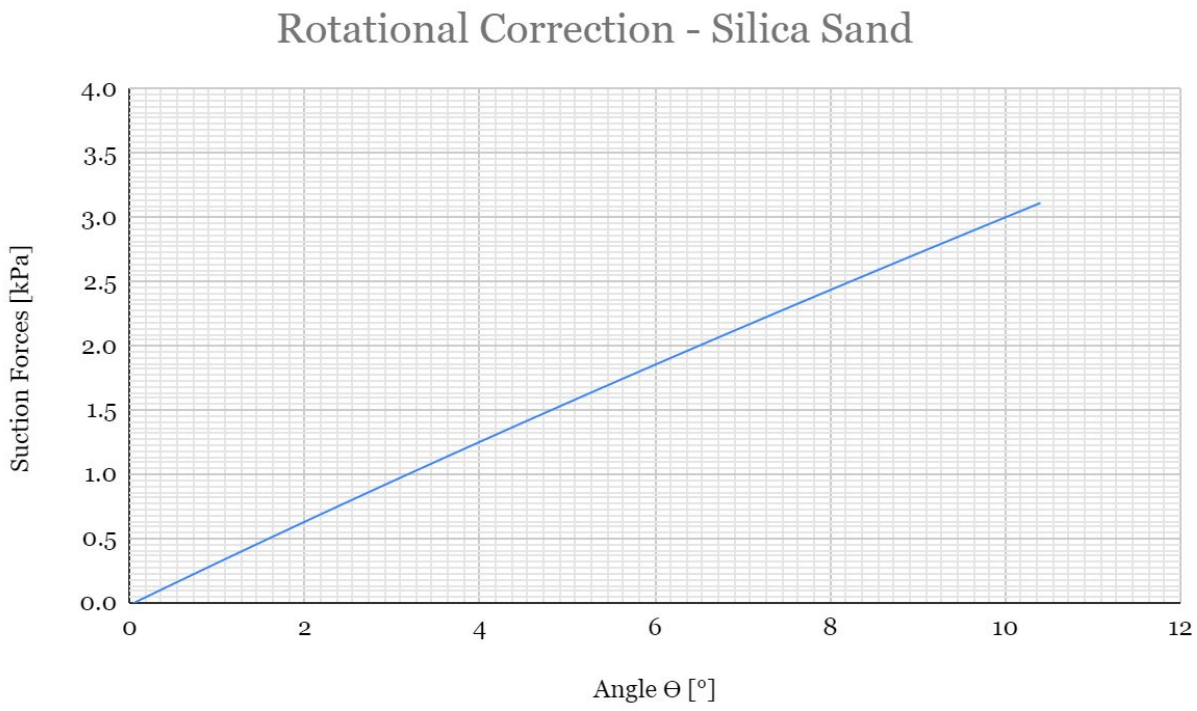

Figure 18. Required Suction Force s to correct a specific angle in Silica sand.

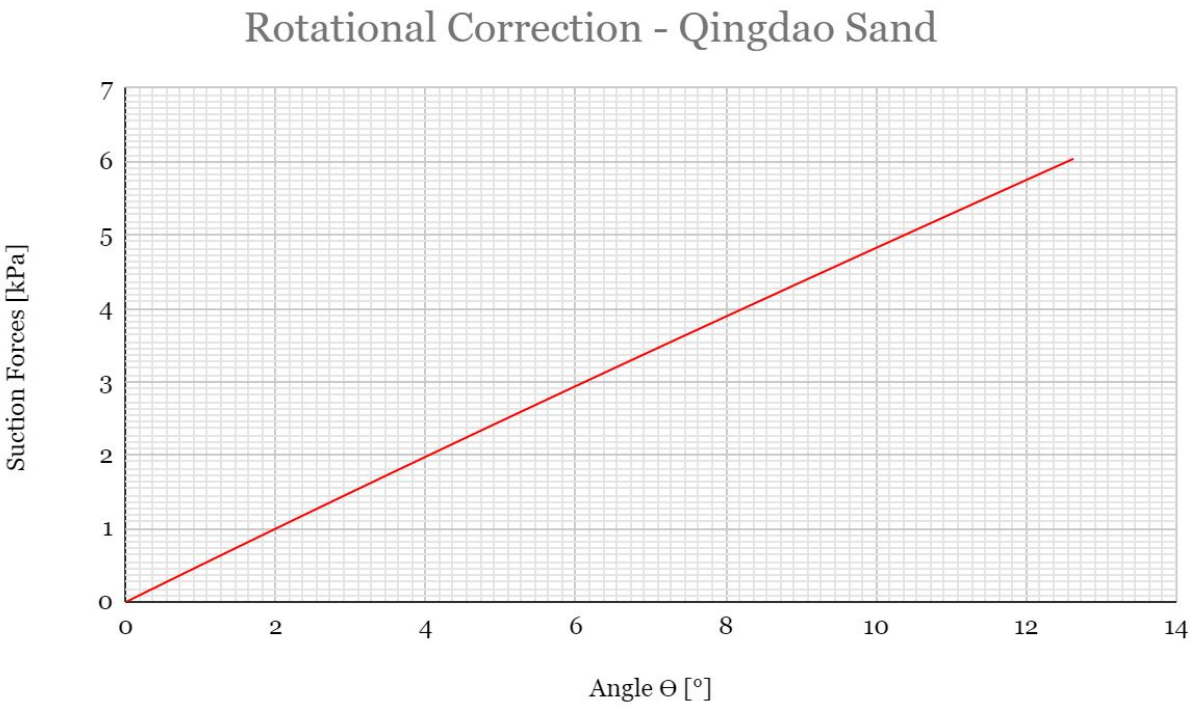

Figure 19. Required Suction Force s to correct a specific angle in Qingdao sand.

7.4 Holding Capacity - Cohesive soils

Equations 23, 24 and 25 will be used to calculate the theoretical undrained holding capacity of the Ocean Foundation in cohesive soils. Table 10 displays an overview of the values that will be used in the aforementioned equations. Here, D_r denotes the aforementioned diagonal length, L_c denotes the skirt length of the circular caissons, and L_r denotes the skirt length of the square- and trapezoidal caissons.

To calculate the weight of the soil plug, the volume of the caissons is required. The volume of the square caissons in the middle was calculated to be 72 liters. Each trapezoidal-shaped caisson has a volume calculated to be 139.37 litres. Collectively the rectangular caissons have a volume of 629.48 liters, which will be denoted by the variable V_r. The volume of a single circular caisson will, in turn, be denoted by the variable V_c.

Table 10. Skirt lengths and diameters of the suction caissons.

Description	***Symbol***	***Unit***	***Value***
Weight of the structure	W_c	N	9328,6
Circular Caisson Properties			
Diameter - Outside	D_o	m	0.508
Skirt length	L_c	m	0.5
Volume	V_c	m^3	0.0970
Rectangular Caissons Properties			
Overall diameter	D_r	m	2.32043
Skirt length	L_r	m	0.2
Volume	V_r	m^3	0.62948

The properties of Kaolin clay and Qiantang River silt will be taken from table 4. For both Kaolin clay and Qiantang River silt, the values of Q_{so}, Q_b and W_s were calculated and summed up into the variable Q_{sum}. These values were calculated separately for one single circular caisson, as well as the square- and the trapezoidal caissons together. The undrained holding capacity Q is then the sum of Q_{sum} and the weight of the structure, W_c, as shown in equation 23. The theoretical value of the undrained pullout capacity Q in Kaolin clay is given in table 11, whereas the value of Q for Qiantang River silt is given in table 12. All values in these tables are shown in kilonewton.

Table 11. Undrained pullout capacity in Kaolin clay

Kaolin clay	Q_{so}	Q_b	W_s	Q_{sum}
Circular	1.596	5.108	0.695	7.399
Square + Trapezoidal	2.916	106.568	4.513	113.997
			Total	143.593
Total undrained holding capacity *Q*				152.922

Table 12. Undrained pullout capacity in Qiantang River silt

Qiantang River silt	Q_{so}	Q_b	W_s	Q_{sum}
Circular	2.394	7.661	0.856	10.911
Square + Trapezoidal	4.374	159.852	5.554	169.780
			Total	213.424
Total undrained holding capacity *Q*				222.753

7.5 Holding Capacity - Non-cohesive soils

Equations 27 and 28 can be used to determine the theoretical undrained holding capacity in the non-cohesive soils studied in this research: silica sand and Qingdao sand. The properties of Silica sand and Qingdao sand are taken from table 7. The properties of the caissons that will be used in these equations are taken from table 10.

The results for Silica sand are shown in table 13, whereas the results for Qingdao sand are shown in table 14. All values in these tables are shown in kilonewton. The resistance forces and the weight of the soil plugs will be calculated separately for the circular caissons and the rectangular caissons, after which they will be summed up into the variable R_{sum}. The undrained holding capacity H_c is then the sum of R_{sum} and the weight of structure, W_c, as shown in equation 28.

Table 13. Undrained holding capacity in Silica sand

Silica sand	$R_{s(OS)}$	$R_{s(IS)}$	W_s	R_{sum}
Circular	0.746	0.746	0.581	2.0728
Square + Trapezoidal	0.550	0.550	3.772	4.873
			Total	13.165
Total undrained holding capacity H_c				22.493

Table 14. Undrained holding capacity in Qingdao sand

Qingdao sand	$R_{s(OS)}$	$R_{s(IS)}$	W_s	R_{sum}
Circular	1.269	1.269	0.989	3.528
Square + Trapezoidal	0.937	0.937	6.421	8.294
			Total	22.406
Total undrained holding capacity H_c				31.735

8. Conclusion

This research was performed to study the performance of the current Ocean Grazer prototype in different oceanic soils. Due to the COVID-19 circumstances present from the start of the year 2020 until the completion of this research, literature has been primarily used to generate results. Four different oceanic soils were studied in this research, two of which are cohesive soils and two of which are non-cohesive soils. These soils are Kaolin clay, Qiantang River silt, Silica sand and Qingdao sand. Literature regarding the composition of the ocean floor in the North Sea was used to determine which soil types would most likely be encountered during future testing. Consequently, the four aforementioned soils were selected to best represent soils that would be encountered in the North Sea. This study has analysed the performance of the Ocean Grazer prototype during installation and during operation.

The effect of soil composition on the initial installation depth of the prototype has been modelled by plotting the stress present in the system against the depth that the tip of the caisson skirt would reach. It can be concluded that in standard marine sand, such as Silica sand, no issues will occur. In denser sand with finer grains, such as Qingdao sand, the self-weight installation depth is notably smaller, however no further issues occur. In common clay with relatively fine grains, such as Kaolin clay, it can be concluded that no issues occur. In Qiantang River silt it can be concluded that, due to the high undrained shear strength of the soil and the high effective angle of friction, no self-weight penetration is possible. This prevents the creation of a pressure seal, which prevents further installation.

The suction forces required to fully install the Ocean Grazer prototype have been modelled as well. It can be concluded that in both Kaolin clay and Silica sand, no issues will occur during suction-assisted installation. In Qingdao sand, increased resistance results in a higher required suction force. This elevated suction force will theoretically cause piping during the last 12mm of installation. In Qiantang River silt, the theoretical required suction force has been modelled as well, despite the aforementioned issue during self-weight installation. This suction force is notably higher than the required suction force for other soils, due to the increased resistance of the soil. The reverse bearing capacity problem does not occur even in Qiantang River silt, indicating that theoretically, no soil should flow into the caisson. However, due to previously mentioned issues, installation in cohesive soils with high undrained shear strength and a high internal angle of friction is not recommended.

The prototype's ability to correct its rotation if placed on uneven soil was tested. Due to the design of the prototype, it can initially be concluded that the prototype can only correct smaller angles. Currently, only the four circular caissons found on the corners of the prototype will have independent suction pumps, therefore only these caissons could theoretically correct an angle. In Qiantang River silt, this angle is the largest as it is unable to penetrate the soil under self-weight, however as mentioned previously, it is highly unlikely installation in this soil will be possible. In all other soil, the current prototype can only correct a relatively small angle,

therefore it can be concluded that the prototype's ability to correct its angle and become level is poor.

The theoretical holding capacity of the prototype in each soil was determined. In these calculations, the rectangular caissons that the prototype offers were taken into account, as these caissons' primary function is to increase the holding capacity of the system. The holding capacity was determined through a total-stress approach. In other words, the theoretical amount of upward force the prototype can withstand once fully installed was calculated. It can be concluded that in cohesive soils the holding capacity of the system is very high, due to the inherent cohesion of the soil. In non-cohesive soils, the holding capacity is notably smaller. This could indicate that indeed the prototype performs much better in cohesive soils, or it could indicate that the methodology used to determine the holding capacity for cohesive soils in this study is not applicable for the current prototype design. Therefore, it is strongly recommended that holding capacity tests are performed experimentally.

Insights into the prototype's performance during cyclic loading could not be gathered through literature. Based on the literature discussed in this study, performance during cyclic loading is to be determined experimentally. Due to a lack of facilities, this information could not be gathered for this research. Therefore, it is recommended that cyclic-loading tests are performed on scaled models so that the loss of holding capacity over time can be determined.

9. Discussion

As mentioned previously, the circumstances surrounding the COVID-19 situation as of the year 2020 have prevented access to facilities that would facilitate physical experiments. As such, all results gathered in this study have been determined through literature. By simulating experiments as found in relevant literature, the results presented in this study have been validated to the best of the author's ability. Regardless, it is strongly recommended that physical experiments are performed with a model of the current prototype, so that the results gathered in this study can be used as a tool for comparison.

The circumstances surrounding the COVID-19 situation similarly prevented the gathering and testing of soil from the North Sea. Therefore, soils had to be selected based on literature. Through an analysis of soils of the North Sea, a multitude of soils were collected that best represented the most common soil types present in the North Sea. However, it can reasonably be assumed that there will be discrepancies between the soils used in this study and the soils commonly found in the North Sea. Therefore, it is recommended that soil samples from the North Sea are collected and tested as soon as the current circumstances allow it, so that experiments with these soils can be conducted.

In order to simplify the set of equations used to determine the self-weight installation depth and required suction forces for full installation, the results related to these equations do not include the rectangular caissons. The main purpose of these rectangular caissons is to increase the holding capacity of the system, however it can be reasonably assumed that the added friction of the caisson walls will increase the total stress during installation, which could result in a lower self-weight penetration depth and higher suction-force requirements. Similarly, the effects of the rectangular caissons were not included when determining the prototype's ability to correct its rotation. A lower self-weight installation depth due to higher friction forces would result in a bigger angle that could be corrected, however a higher suction-force requirement.

Bibliography

Abuhajar, O., Naggar, E., Hesham, M. and Newson, T. (2010) "Review of Available Methods for Evaluation of Soil Sensitivity for Seismic Design", International Conferences on Recent Advances in Geotechnical Earthquake Engineering and Soil Dynamics. 27.

Ahn, J., Lee, H. and Kim, Y.-T. (2014) "Holding Capacity of Suction Caisson Anchors Embedded in Cohesive Soils Based on Finite Element Analysis," 38(15), pp. 1541–1555. doi: 10.1002/nag.2268.

Bockelmann, F.-D. *et al.* (2018) "Mapping Mud Content and Median Grain-Size of North Sea Sediments - a Geostatistical Approach," 397, pp. 60–71. doi: 10.1016/j.margeo.2017.11.003.

Bolton & C.k. Lau (1993) "Vertical Bearing Capacity Factors for Circular and Strip Footings on Mohr-Coulomb Soil, Canadian Geotechnical Journal, 30(6), Pp 1024-1033" (1994), 31(4), pp. 206–206. doi: 10.1016/0148-9062(94)91186-X.

Byrne, B. W. (2000) "Investigations of Suction Caissons in Dense Sand." PhD thesis.

Byrne, B. W. *et al.* (2002) "Suction Caisson Foundations for Offshore Wind Turbines," 26, pp. 145–156.

Chen, W. (2007) "Uplift Capacity of Suction Caissons Under Sustained and Cyclic Loading in Soft Clay," 133(11), pp. 1352–1363. doi: 10.1061/(ASCE)1090-0241(2007)133:11(1352).

Coduto, Donald P. (2001) "Foundation design : principles and practices" (2nd ed.). Upper Saddle River, N.J.: Prentice Hall. ISBN 0135897068. OCLC 43864336

Colliat, J.-L. *et al.* (1998) "Design and Installation of Suction Anchor Piles at Soft Clay Site," 124(4), pp. 179–188. doi: 10.1061/(ASCE)0733-950X(1998)124:4(179).

Das, Braja M (2007) "Principles of foundation engineering" (6th ed.). Toronto, Ontario, Canada: Thomson. ISBN 978-0495082460. OCLC 71226518

van Dijk, B. (2018) "Design of Suction Foundations," 19(8), pp. 579–599. doi: 10.1631/jzus.A1700465.

Harireche, O., Mehravar, M. and Alani, A. M. (2014) "Suction Caisson Installation in Sand with Isotropic Permeability Varying with Depth," 43, pp. 256–263.

Houlsby, G. T., Byrne, B. W. (2005) "Design procedures for installation of suction caissons in clay and other materials," Proceedings of the Institution of Civil Engineers - Geotechnical Engineering. 158. 75-82. doi: 10.1680/geng.2005.158.2.75.

Hung, L. C., Lee, S., Tran, N. X., Kim, S. (2017) "Experimental investigation of the vertical pullout cyclic response of bucket foundations in sand," Applied Ocean Research, Volume 68, pp. 325-335, ISSN 0141-1187, doi:10.1016/j.apor.2017.06.006.

International Organization for Standardization. (2002). “ISO 14688-1:2002 Geotechnical investigation and testing — Identification and classification of soil — Part 1: Identification and description”: ISO

Iskander, M., El-Gharbawy, S., Olson, R. (2011). “Performance of suction caissons in sand and clay”. Canadian Geotechnical Journal. 39. 576-584. 10.1139/t02-030.

Jostad, H., Andersen, K. (2015) “Calculation of undrained holding capacity of suction anchors in clays”. Frontiers in Offshore Geotechnics III, pp. 263-268. doi:10.1201/b18442-21.

Li, D. *et al.* (2015) “Capacity of Modified Suction Caissons in Marine Sand Under Static Horizontal Loading,” 102, pp. 1–16. doi: 10.1016/j.oceaneng.2015.04.033.

van der Loo, K. (2020) “Laboratory experiments on the technical feasibility of the Ocean Battery suction foundation in sand,” University of Groningen FSE, Bachelor Thesis

McLaws, I. J. (1971). “Uses and specifications of silica sand”. Edmonton, Alta, Research Council of Alberta.

Paramor, O.A.L., Allen, K.A., Aanesen, M., Armstrong, C., Hegland, T., Le Quesne, W., Piet, G.J., Raakær, J., Rogers, S., van Hal, R., van Hoof, L.J.W., van Overzee, H.M.J., and Frid C.L.J. (2009) “MEFEPO North Sea Atlas”. University of Liverpool. ISBN 0 906370 60 4

van der Reijden, KJ, Koop, L, O'Flynn, S, Garcia, S, Bos, O, van der Sluis, C, Maaholm, DJ, Herman, PMJ, Simons, DG, Olff, H, Ysebaert, T, Snellen, M, Govers, LL, Rijnsdorp, AD & Aquilar, R (2019) “Discovery of Sabellaria spinulosa reefs in an intensively fished area of the Dutch Continental Shelf, North Sea”, Journal of Sea Research, vol. 144, pp. 85-94.doi: 10.1016.2018.11.008

Standard Practice for Classification of Soils for Engineering Purposes (Unified Soil Classification System) (2017), ASTM D2487-17e1, ASTM International, West Conshohocken, PA. doi: 10.1520/D2487-17E01

Sun, Shulin & Xu, Huifang. (2007) “Determining the Shear Strength of Unsaturated Silt” 10.1007/3-540-69873-6_19.

Suzuki, M. *et al.* (2017) “Ring shear characteristics of discontinuous plane”, Soils and Foundations, Volume 57, Issue 1, Pages 1-22,ISSN 0038-0806, doi:10.1016/j.sandf.2017.01.001.

Villalobos, F. A., Byrne, B.W., Houlsby, G. T. (2010) “Model testing of suction caissons in clay subjected to vertical loading,” Applied Ocean Research, Volume 32, Issue 4, pp. 414-424. ISSN 0141-118, doi: 10.1016/j.apor.2010.09.002.

Wachowski, Łukasz. (2016). “The Pull-out Capacity of Suction Caissons in Model Investigations.”, Archives of Hydroengineering and Environmental Mechanics. Vol. 63. 157-171. 10.1515/heem-2016-0010.

Wang, Y. *et al.* (2018) “Large Deformation Finite Element Analysis of the Installation of Suction Caisson in Clay,” 36(8), pp. 883–894. doi: 10.1080/1064119X.2017.1395496.

Wang, Lizhong & Yu, Luqing & Guo, Zhen & Wang, Zhenyu. (2013). “Seepage Induced Soil Failure and its Mitigation During Suction Caisson Installation in Silt.”, Journal of Offshore Mechanics and Arctic Engineering. 136. 011103. 10.1115/1.4025677.

Zhang, Y., Li, D. and Gao, Y. (2017) “Model Tests on Installation and Extraction of Suction Caissons in Dense Sand,” 35(7), pp. 921–929. doi: 10.1080/1064119X.2016.1259698.

Zhou, H. and Randolph, M. F. (2006) “Large Deformation Analysis of Suction Caisson Installation in Clay,” 43(12), pp. 1344–1357. doi: 10.1139/t06-087.